



This is to certify that the

thesis entitled

DYNAMIC AUGMENTATION OF DISSIPATIVE ALGEBRAIC LOOPS

presented by

Peter L. Graf

has been accepted towards fulfillment of the requirements for

Masters degree in Mech. Engr.

R.C.Kpenberg

Date 5/21/81

O-7639

DYNAMIC AUGMENTATION OF DISSIPATIVE ALGEBRAIC LOOPS

Ву

Peter Leo Graf

A THESIS

Submitted to
Michigan State University
in partial fulfillment of the requirements
for the degree of

MASTER OF SCIENCE

Department of Mechanical Engineering

ABSTRACT

DYNAMIC AUGMENTATION OF DISSIPATIVE ALGEBRAIC LOOPS

Ву

Peter Leo Graf

In the design and simulation of dynamic systems, an explicit state-space representation of the equation set is preferred. For strictly linear systems, the explicit state-space representation is, in theory, readily obtained. On the other hand, the uncooperative nature of nonlinear systems may prevent the derivation of an explicit state-space representation. The incidence of algebraic loops contributes to this difficulty. Their origin may result from the interaction between system topology and nonlinear dissipative fields. Within the framework of the bond-graph approach, a numerically-oriented procedure for dealing with dissipative algebraic loops is presented and illustrated by examples.

ACKNOWLEDGEMENTS

At this time, I wish to extend my sincere gratitude to my advisor, Dr. Ronald Rosenberg, for his inspiration and guidance throughout my thesis research. To my family, especially my mother and father Martha and Otto Graf, I remain eternally grateful for their unwaivering love and support for me. Also, I thank Mrs. Jan Swift for the speedy and efficient typing of this manuscript.

TABLE OF CONTENTS

LIST	OF T	ABLESv
LIST	OF F	IGURESvi
KEY '	TO SY	MBOLSviii
1.0	INTR	ODUCTION1
	1.1 1.2 1.3 1.4	Techniques for Lumped Parameter System Description
2.0	THE	BOND GRAPH METHOD AND ALGEBRAIC LOOPS7
	2.1	Bond Graphs7
		2.1.1 An Example7
	2.2	Identification of Algebraic Loops in Bond Graphs
3.0	A SO	LUTION METHOD BASED ON DYNAMIC AUGMENTATION17
	3.1	The Method of Dynamic Augmentation17
		3.1.1 The Procedure18
	3.2	Minimum-Maximum Order Augmentation21
		3.2.1 Example 223
	3.3	The Secondary Dynamics Problem23
		3.3.1 Linear Dissipative Fields
	3.4	The Solution Flowchart 46

4.0	NUME	RICAL EXAMPLES52
	4.1 4.2	Example 1
5.0	CONC	LUSIONS66
	5.1 5.2 5.3	The General Problem Structure
APPE	NDIX	A170
APPE	NDIX	A274
REFE	RENCE	S76



LIST OF TABLES

TABLE 3-	-1 Simulation	Data37
TABLE 4-	-l Simulation	Data55
TABLE 4-	-2 Eigenvalue	Approximation59
TABLE 4	-3 Simulation	Data61
TABLE 4-	-4 Eigenvalue	Approximation62



LIST OF FIGURES

FIGURE	2-1.	A FIELD REPRESENTATION FOR A BOND GRAPH8
FIGURE	2-2.	A BOND GRAPH EXAMPLE9
FIGURE	2-3.	A CAUSALLY COMPLETE BOND GRAPH12
FIGURE	2-4.	THE PARTITIONED BOND GRAPH CONCEPT15
FIGURE	2-5.	A PARTITIONED BOND GRAPH16
FIGURE	3-1.	A DYNAMICALLY AUGMENTED SUBGRAPH19
FIGURE	3-2.	AN ELECTRICAL ANALOG20
FIGURE	3-3.	THE PREFERRED DYNAMIC AUGMENTATION22
FIGURE	3-4.	A BOND GRAPH EXAMPLE24
FIGURE	3-5.	POSSIBLE DYNAMIC AUGMENTATIONS25
FIGURE	3-6.	EIGENVALUE SEPARATION31
FIGURE	3-7.	AN AUGMENTED SUBGRAPH35
FIGURE	3-8.	CASE 138
FIGURE	3-9.	CASE 239
FIGURE	3-10.	CASE 340
FIGURE	3-11.	CASE 441
FIGURE	3-12.	CASE 542
FIGURE	3-13.	SOLUTION PROCESS DIAGRAM51
FIGURE	4-1.	CASE 156
FIGURE	4-2.	CASE 257
FIGURE	4-3.	CASE 358
FIGURE	4-4.	DISSIPATIVE FUNCTIONS FOR EXAMPLE 263



FIGURE 4-5.	CASE 164
FIGURE 4-6.	CASE 265
FIGURE 5-1.	THE PROBLEM STRUCTURE

KEY TO SYMBOLS

X	- a vector
*	- time derivative of a vector
x ~	- a steady state vector
t_d	- the global system time variable
$x_{t_d}(0)$	- initial conditions for a subgraph at the global time $\boldsymbol{t}_{\boldsymbol{d}}$
k _{opt}	- an optimal parameter
$G_{\overline{D}}$	- a dynamic subgraph
G_S	- a static subgraph
λ	- an eigenvalue
det[S]	- the determinant of the S matrix

1.0 INTRODUCTION

1.1 Techniques for Lumped Parameter System Description

In approaching a dynamics problem, one must first define the system and its environment. Subsequently, the various processes within the system and interactions between the system and its environment must be modeled. At this point, the physical system dynamicist has at his disposal several techniques to effect a mathematical model. Among these are Newtonian methods, Lagrangian methods, network and circuit methods, and bond-graph methods [7, 8, 9, 1].

1.2 State-Space Representation

In the design and simulation of dynamic systems, an explicit state-space representation is desirable. Much work has been directed toward the development of efficient numerical algorithms for application to this form. These numerical schemes can be separated into two basic categories: 1) direct numerical integration algorithms such as Runge-Kutta or predictor-corrector methods [2], and 2) transition matrix generation by techniques such as the Peano-Baker series [10].

For linear systems, the well known form is:

$$\dot{x} = Ax + Bu \tag{1-1}$$



where x is the state vector of dimension n, u is the input vector of dimension m, and A and B are matrices of appropriate dimensions.

The analogous explicit representation for nonlinear systems is

$$\dot{x} = \phi(x, u) \tag{1-2}$$

where x and u are defined as before and ϕ is a nonlinear vector function.

1.3 The Incidence of Algebraic Loops

The contrary nature of the nonlinear dynamics problem often renders the formulation of an explicit state-space representation intractable. One such difficulty, preventing the desired representation, may be traced to the incidence of algebraic loops (coupled algebraic equations) in the system equation set. Particularly, the existence of these algebraic loops may be a consequence of the interaction between the system structure (topology) and dissipative mechanisms in the system.

An example of the equation set for a general second order single input dynamic system containing an algebraic loop is presented below. The state vector x and input vector u are of dimension 2 and 1 respectively. The intermediate variables are denoted by v and w.

$$\dot{x}_1 = \phi_1 (x_1, x_2, v, w, u)$$
 (1-3)

$$\dot{x}_2 = \phi_2 (x_1, x_2, v, w, u)$$
 (1-4)



$$v = \gamma_1 (x_1, x_2, v, w, u)$$
 (1-5)

$$w = \gamma_2 (x_1, x_2, v, w, u)$$
 (1-6)

In this example, the intermediate variables v and w are coupled in an arbitrary manner with each other, the state variables, and the input u. Given either γ_1 or γ_2 to be a nonlinear function could suffice to prevent an explicit state-space form for this system.

In general, the incidence of nonlinear algebraic loops in the system equation set will typically prevent subsequent reduction of the system equation set to an explicit state-space form.

1.4 Some Previous Work on the Problem of Algebraic Loops

Many good simulation programs exist that will diagnose the incidence of algebraic loops in the equation set. Among these are CSMP, CSSL, DARE, and SCEPTRE [3, 4, 5, 6]. Operationally, a loop diagnostic occurs following the equation sorting process. In this process, as the system equation set is manipulated, mutual algebraic dependencies are identified. Typically, execution of the program is terminated and appropriate modifications must be performed.

Both CSMP III and CSSL IV employ similar algorithms to circumvent existing algebraic loops. The success of the algorithm hinges on the expression of the algebraic loop equation in the scalar form

$$z = f(z) \tag{1-7}$$



A preprogrammed iterative solution algorithm is then available to deal with the loop equation.

Having expressed the loop equation in the desired form of equation (1-7), the variable of interest is redefined as:

$$z = IMPL (ZO, ERROR, FOFZ)$$
 (1-8)

where

During simulation, this algorithm must be accessed on each derivative call - perhaps 2-5 times per DT step.

Several major limitations are intrinsic to this method:

- 1) The definition of f(z) may not be unique (e.g. the user may solve for z=f(z) in several ways). Moreover, a solution may not be unique. Convergence to a particular solution could depend on the initial guess as well as the particular definition of f(z).
- 2) The implicit function routine does not allow nested implicit loops (i.e. coupled nonlinear equations).



The circuit analysis program SCEPTRE approaches the problem of algebraic loops by the implementation of a computational delay. Ideally, every variable quantity in a system is updated at the start of each time step using the updated state variables and time. If, however, an implicit loop is present, the program will use the value of the independent variable that existed at the previous time step. Again, a functional form similar to equation (1-7) is assumed.

The error introduced is dependent on the character of the nonlinearity in the functional dependence and the time step.

Error may become serious in some cases. At any rate, a diagnostic alerting the user of the computational delay is provided.

Korn and Wait [4] discuss several methods for manipulation of algebraic loops. Mention is made of the solution techniques utilized in CSMP, CSSL software and SCEPTRE software. Another approach offered by Korn and Wait suggests generating functions as solutions of differential equations. For example, if the variable Y is implicitly defined as

$$\psi(x_1, x_2, ..., T; Y) = 0$$
 (1-10)

and is suitably differentiable, it may be introduced as a state variable. The differential equation would be of the form

$$\frac{dY}{dT} = -K \frac{\partial \psi}{\partial Y} \operatorname{sign} \psi \qquad (K > 0)$$
 (1-11)



The solution of equation (1-11) (assuming a reasonable solution exists) satisfies a steepest-descent minimization of the function

$$F(x_1, x_2, ..., T; Y) = |\psi(x_1, x_2, ..., T; Y)|$$
 (1-12)

The correct value Y(0) must be established by some type of iteration and K must be chosen by trial and error for best accuracy [4].

The aforementioned procedure includes the possible treatment of coupled nonlinear equations; however, the desired explicit form is sensitive to the nature of nonlinear dependencies.



2.0 THE BOND-GRAPH METHOD AND ALGEBRAIC LOOPS

2.1 Bond Graphs

A bond-graph model may be visualized as a schematic of the dynamic energy exchange between components of a system (see Appendix Al for a more extensive discussion). Energy exchange occurs between input, dissipative, and storage fields through the junction structure consisting of bonds and nodes (see Figure 2-1). Bonds represent paths of power flow and nodes are energy conservative junctions that route power flow according to simple algebraic laws. Further enhancement of information for the bondgraph model can be achieved by indicating preferred power orientations on bonds to establish sign convention. Also, through causal augmentation, a signal orientation in an input/output sense can be specified for each bond.

2.1.1 An Example

Consider the two analogous physical systems in Figure 2-2a, b. In Figure 2-2c, the basic structure of the associated bondgraph model is shown. The I-element represents inertial effects in the mechanical system and inductance effects in the electrical system. Compliance and capacitance effects are indicated by the C-element in the mechanical and electrical systems respectively. The R-elements represent energy dissipative effects in both

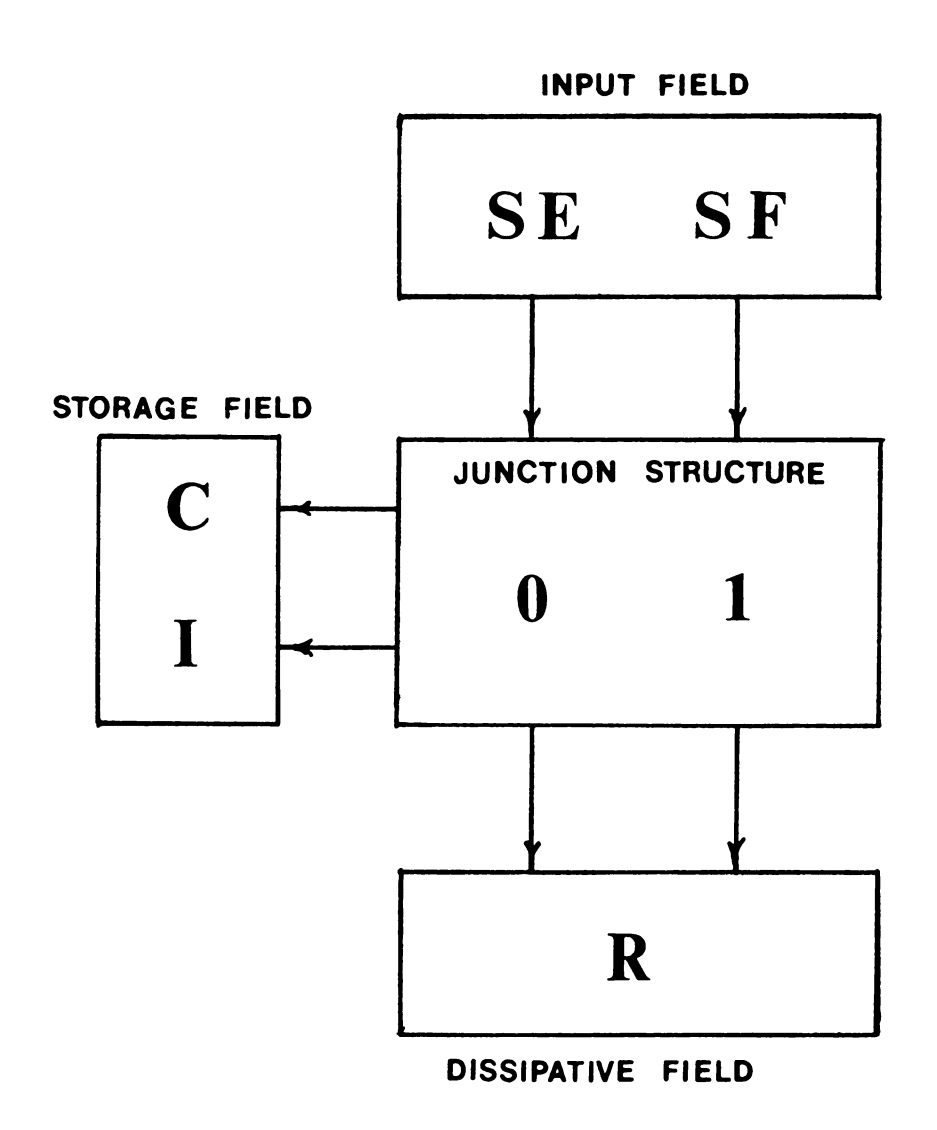
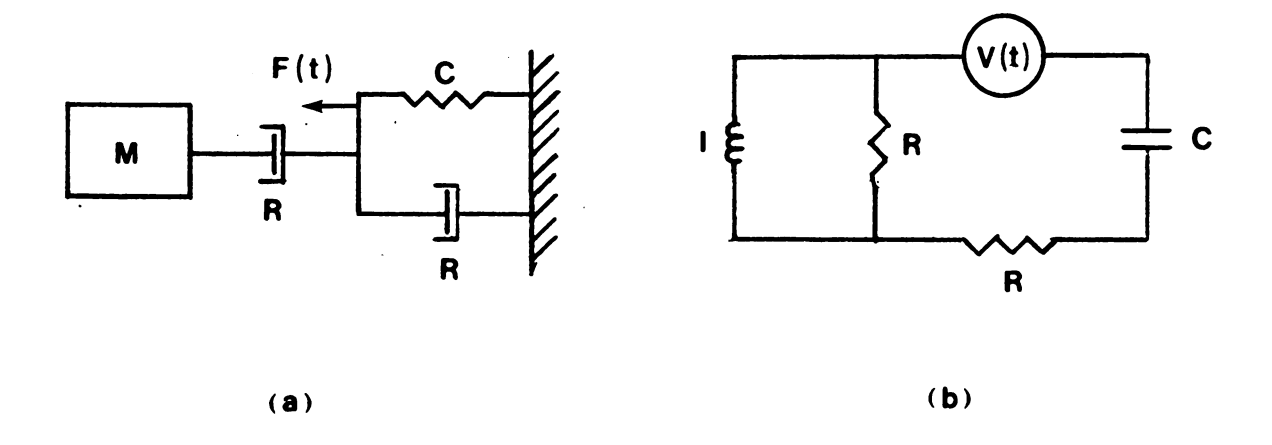
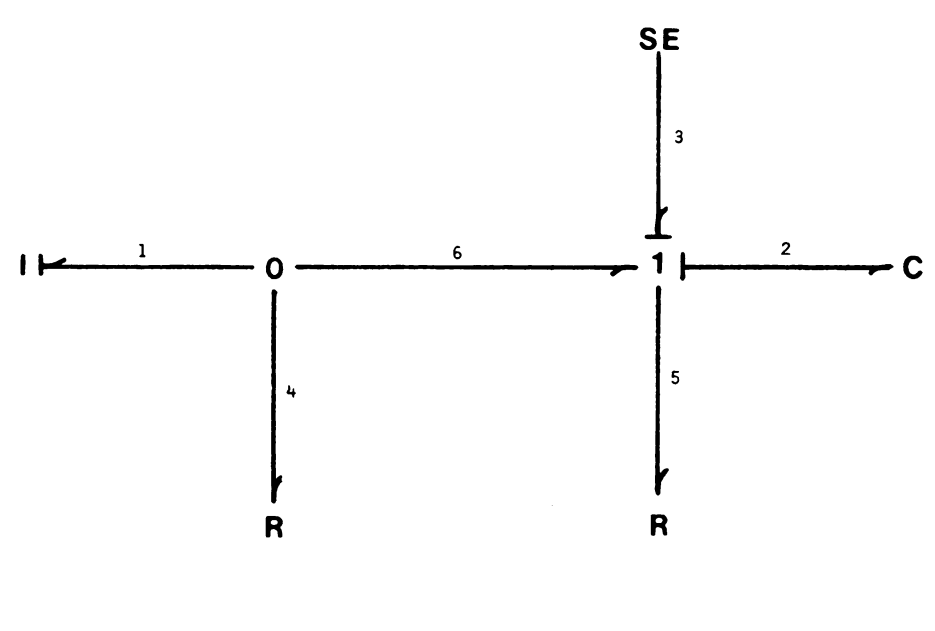


FIGURE 2-1. FIELD REPRESENTATION FOR A BOND GRAPH







(c)

FIGURE 2-2. A BOND GRAPH EXAMPLE

- (a) MECHANICAL SYSTEM
- (b) ELECTRIC CIRCUIT
- (c) THE BOND GRAPH MODEL



systems. The SE-element indicates an imposed effort on the particular system in the form of a force or voltage input.

In this example, there are six bonds; hence, there are six efforts and six flows in addition to the state variables p and x representing the inertance and compliance effects in the system. Consequently, there are 14 equations imposed by the bond-graph structure through node constraints and constituitive relationships. It is desired that the equation set be manipulated to yield an explicit state-space form as follows

$$\dot{p}_1 = g_1 (p_1, x_2, E_3)$$
 (2-1)

$$\dot{x}_2 = g_2 (p_1, x_2, E_3)$$
 (2-2)

At this point, it will be fruitful to discuss the role of causality in the organization of the equation set and as a natural identifier of the existence of algebraic loops.

2.2 Identification of Algebraic Loops in Bond Graphs

As mentioned earlier, assignment of a causal sense to a bond identifies the signal orientation on that bond. For example, bond 3 in Figure 2-2c has a characteristic slash affixed to it. This 'causal stroke' indicates that an effort in the form of a force or voltage is imposed as an input to the system. Likewise, if bond 3 was a current or velocity source, the causal stroke would be switched to the other end of the bond indicating a flow input to the system.



Orderly causal augmentation can be propagated through a bond-graph by following several simple rules [1]. Following this procedure, it may be possible that causality has not been completely extended through the bond-graph.

In the equation sorting process, the occurrence of these acausal graph fragments discloses the existence of algebraic loops.

Reconsidering Figure 2-2c, an acausal condition is apparent on bonds 4, 5, and 6; hence, by the previous supposition, an algebraic loop should arise in the system equation set. Suppose the constitutive relationships for the dissipative elements take the form:

$$f_{\Lambda} = \phi_{\Lambda} \ (e_{\Lambda}) \tag{2-3}$$

$$e_5 = \phi_5 (f_5)$$
 (2-4)

By completing causality on bonds 4, 5 and 6 as shown in Figure 2-3, the implied causal nature of equations (2-3) and (2-4) has been preserved. At this point, the system equation set can be consolidated into the form:

$$\dot{p}_1 = -k_2 x_2 - e_5 - E_3$$
 (2-5)

$$\dot{x}_2 = \frac{P_1}{m_1} - f_4 \tag{2-6}$$

$$f_4 = \phi_4 \left(-k_2 x_2 - e_5 + E_3 \right)$$
 (2-7)



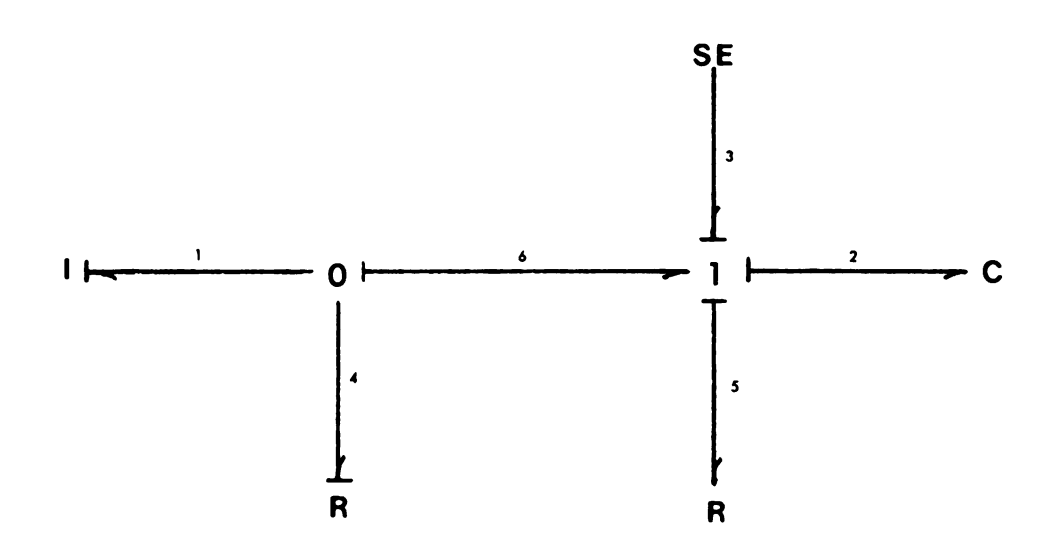
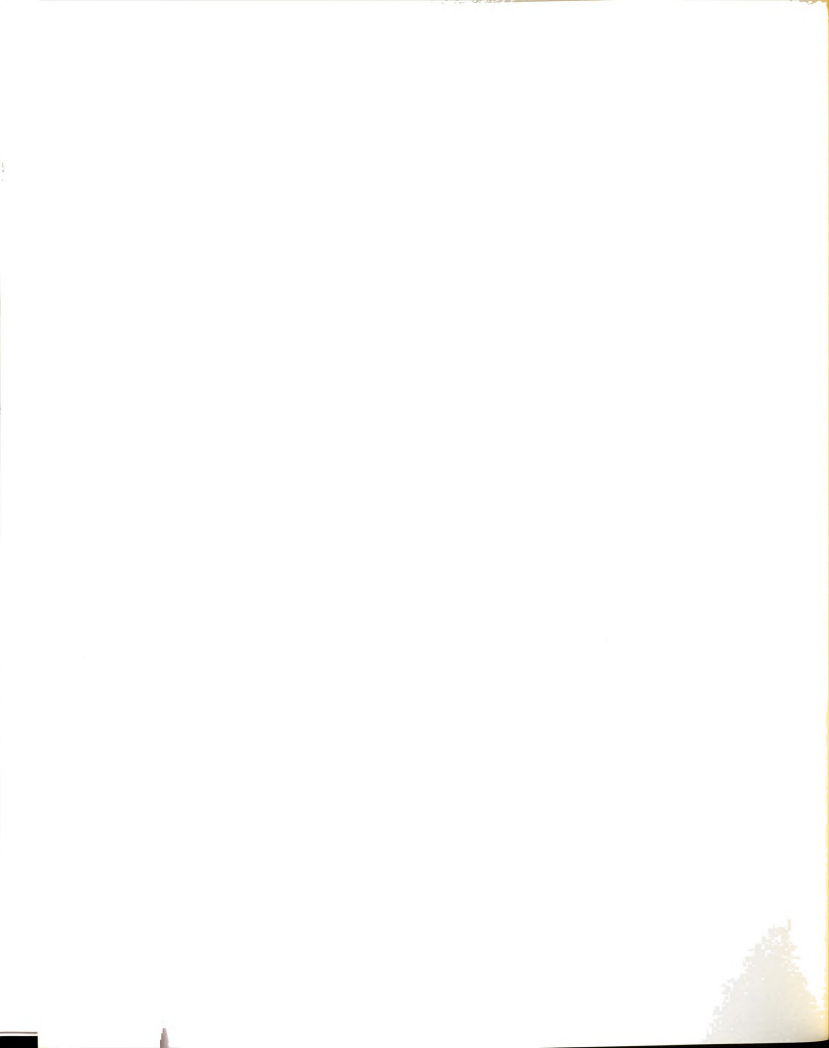


FIGURE 2-3. A CAUSALLY COMPLETE BOND GRAPH



$$e_5 = \phi_5 (p_1/m_1 - f_4)$$
 (2-8)

In this example, the input vector is

$$u = [E_3] \tag{2-9}$$

and the state vector is

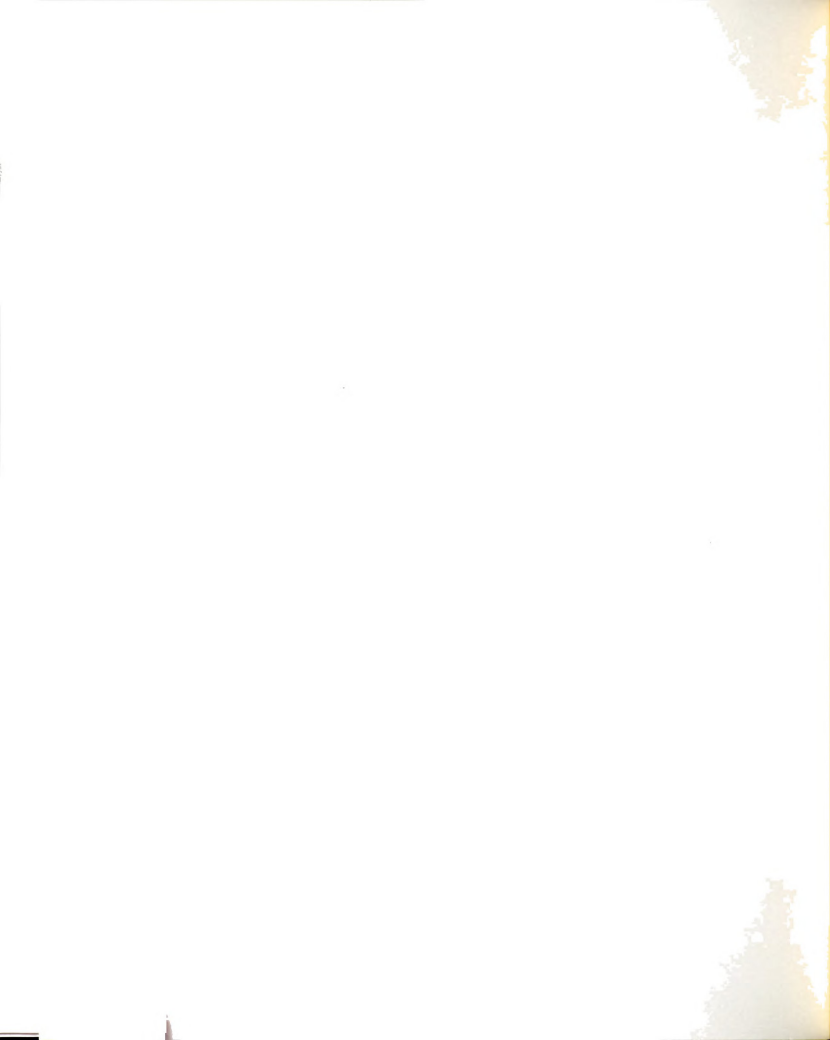
$$\underset{\sim}{\mathbf{x}} = \begin{bmatrix} \mathbf{p}_1 \\ \mathbf{x}_2 \end{bmatrix} \tag{2-10}$$

while f_4 and e_5 are intermediate variables that contribute to the algebraic loop represented in equations (2-7) and (2-8). Consequently, an explicit state space form is predicated on the elimination of f_4 and e_5 from the equation set. In general, explicit analytic solutions of nonlinear coupled equations are difficult if not impossible to achieve.

2.3 Partitioning of Bond Graphs

In the general case of a bond-graph with acausal fragments, partitioning is possible. The bond-graph can be partitioned into causally complete and causally incomplete fragments. The causally complete fragments are, in general, comprised of energy storage fields, dissipative fields, junction structure, and input fields. On the other hand, the acausal fragments will be exclusively dissipative fields with associated junction structure.

For the partitioned bond-graph, it is appropriate to adopt the notation:



 G_{D_i} - ith dynamic sub-graph

$$G_{S_{i}}$$
 - jth static sub-graph

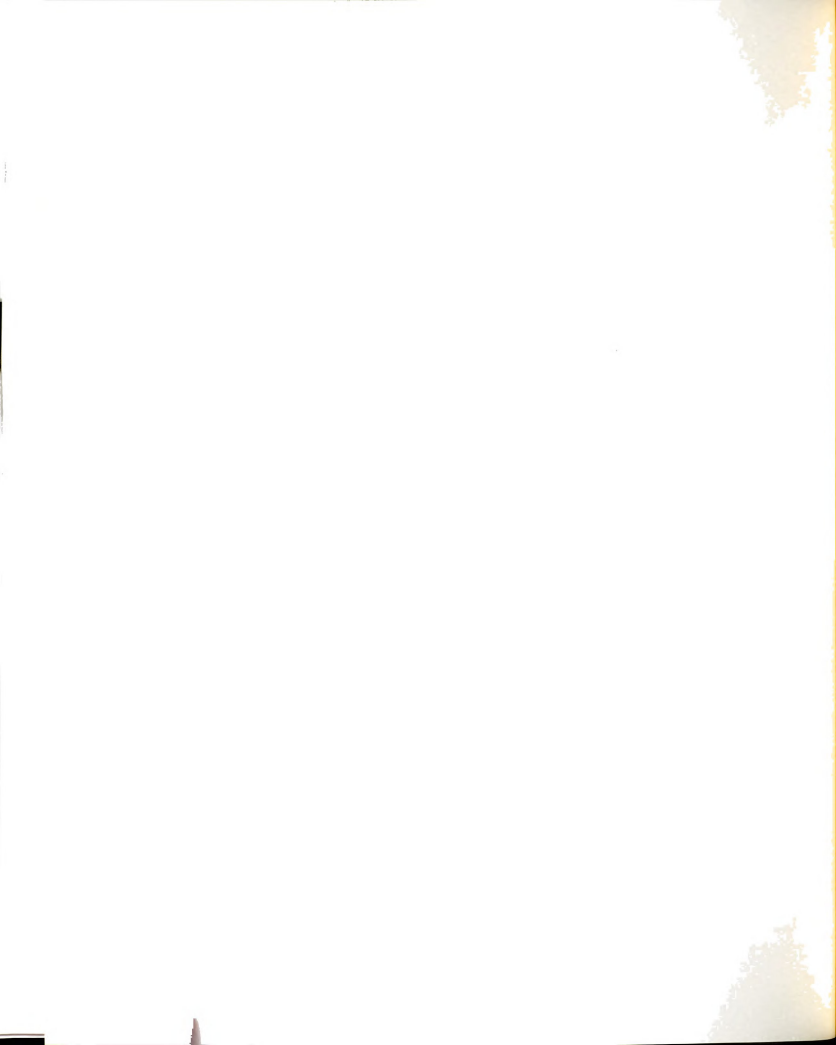
Hence, a bond-graph exhibiting acausal bonds can be partitioned into dynamic and static sub-graphs.* In Figure 2-4, the concept of a partitioned bond-graph is illustrated.

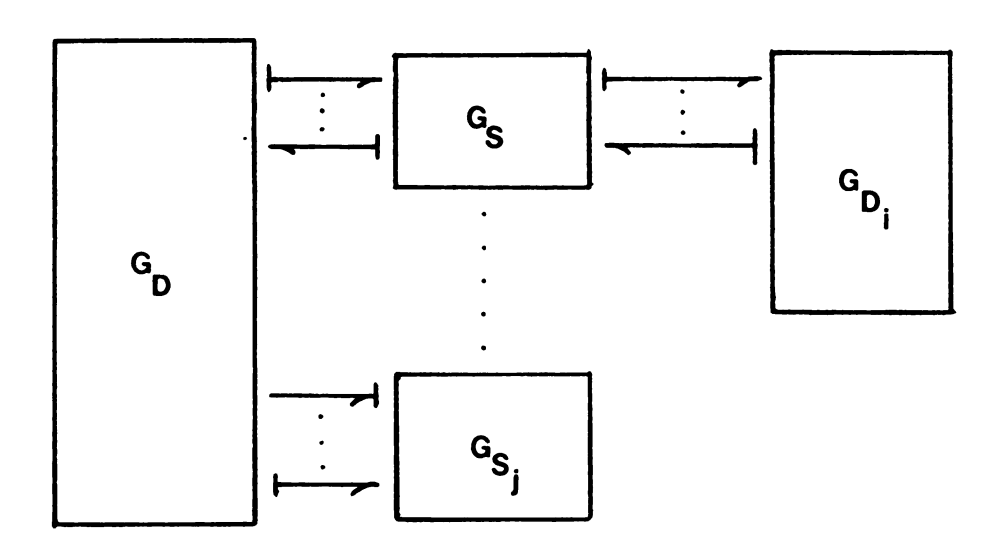
The interaction between the ith dynamic sub-graph and jth static sub-graph may be defined in vector notation. Each sub-graph can be viewed as a separate independent system with both an input and output vector ascribed to it.

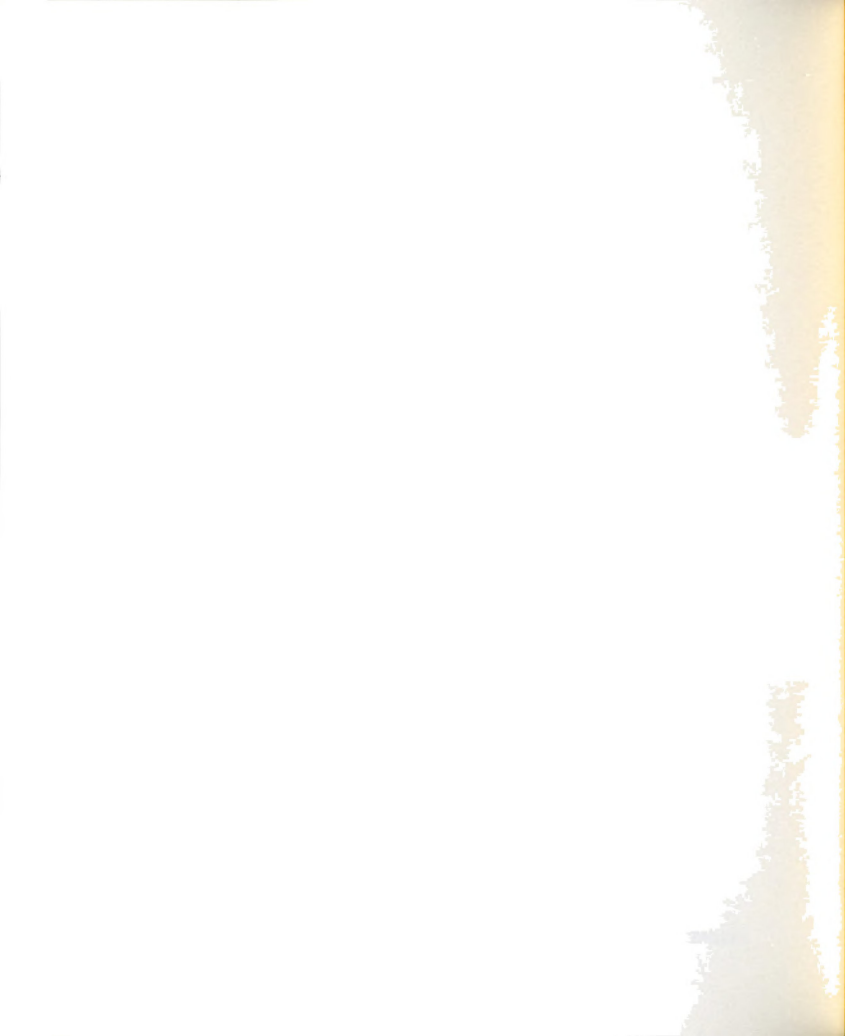
Referring back to Figure 2-2c, it is apparent that the bond-graph exhibits an acausal fragment. In Figure 2-5, the partitioned bond-graph for this example is shown. The static subgraph, G_{ς} , contains the algebraic loop.

In the subsequent chapter, a modification procedure to allow the numerical solution of a bond-graph model containing algebraic loops is introduced. This modification will avoid direct solution of the coupled equations comprising the algebraic loop.

^{*}The term 'static' denotes the absence of dynamic effects.







$$\mathbf{v} = [\mathbf{f}_3] \qquad \mathbf{SE} \\
\mathbf{v} = [\mathbf{e}_3] \qquad \mathbf{G}_{\mathbf{D}_3}$$

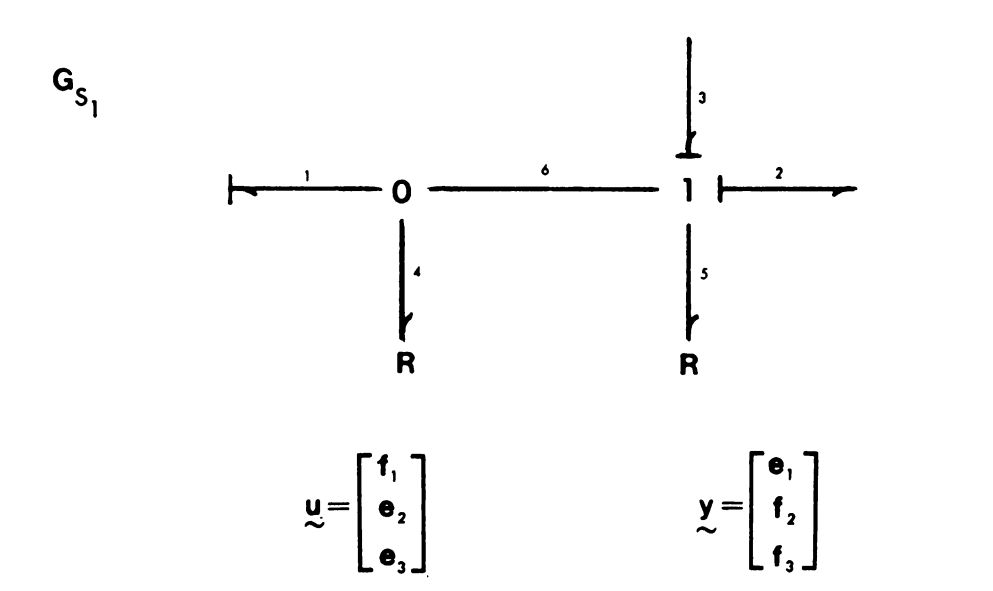


FIGURE 2-5. A PARTITIONED BOND GRAPH

3.0 A SOLUTION METHOD BASED ON DYNAMIC AUGMENTATION

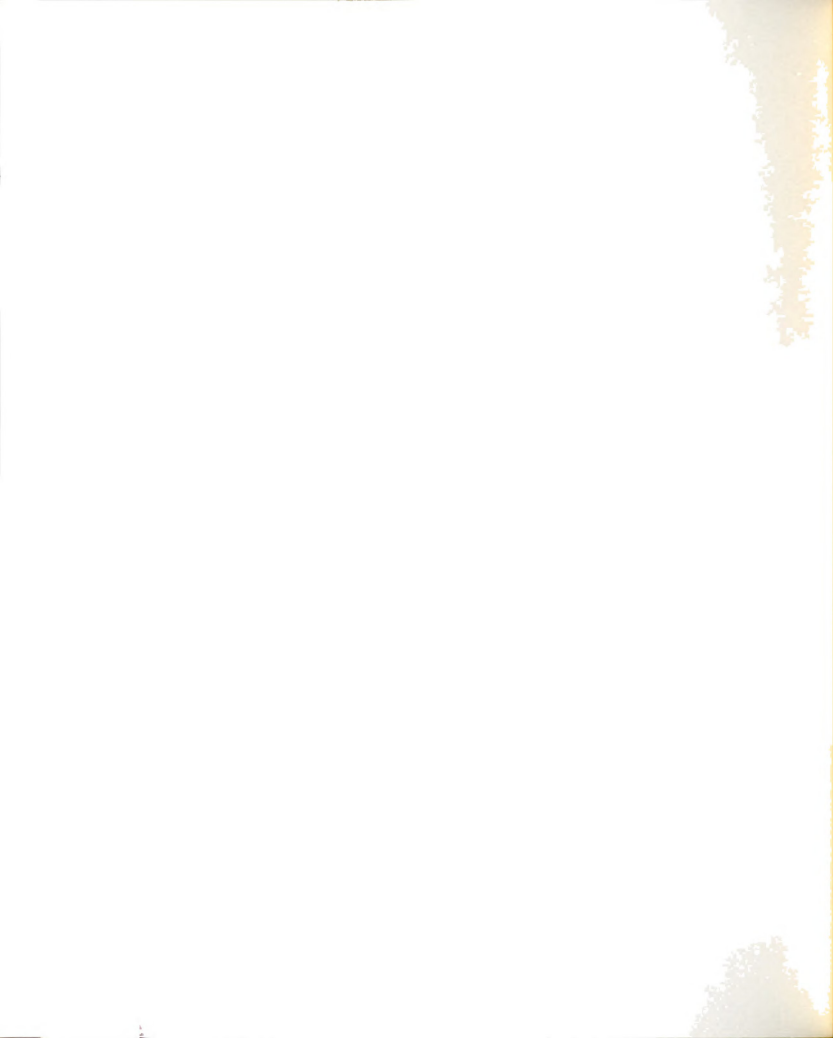
3.1 The Method of Dynamic Augmentation

It is possible to avoid the computationally unwieldy numerical techniques required to solve the coupled nonlinear algebraic equations that may emerge from an algebraic loop. An alternative and perhaps more elegant approach avails itself in the bond graph method. (Such a procedure could also be implemented in a circuit program such as SCEPTRE.)

Reconsider the partitioned bond graph in Figure 2-5. At any time t in a simulation of the system, the dynamic and static subgraphs may be visualized as communicating through mutually shared bonds. Mathematically, the communication linkage is defined in terms of the flow and effort variables associated with the shared bonds. These bond variables can be written in input/output vector notation for each sub-graph.

Suppose that each static sub-graph of a partitioned system was transformed into a dynamic sub-graph by some type of selective dynamic augmentation. In addition, let us postulate that this selective dynamic augmentation will yield a system with the characteristic that at steady state, its output vector will be the same as that of the original unaugmented static sub-graph.

Thus, at time t in the simulation, a dynamic sub-graph $(\mathbf{G}_{\mathrm{D}})$ will define a constant output vector which will serve as inputs



to one or more dynamically augmented sub-graphs (G_S) . The numerically determined steady-state output vector of each G_S will, in turn, describe a set of inputs to the appropriate G_D . Hence, the global system simulation can be achieved in a piecewise fashion.

The details of the solution process implied by this type of structural modification approach will be discussed later. The two important implications of this proposition are:

- 1) Algebraic loop equations are avoided.
- 2) Simulation is effected in a piecewise fashion.

3.1.1 The Procedure

The proposal for the selective dynamic augmentation of a static sub-graph consists of adding I-elements to 1-junctions and C-elements to 0-junctions. The 'I' and 'C' elements are considered to be of a class of linear, conservative, energy storage fields. For example, in Figure 3-1, G_{S_1} from Figure 2-5 has been dynamically augmented. By virtue of the augmentation, a 'new' dynamic system has been posed.

In Figure 3-2, an electrical analog of the 'new' system is pictured. In essence, the static structure of the dissipative problem has been recast into the dynamic realm.

The premise of this transformation maintains that the steadystate output of a dynamically augmented subsystem will satisfy the original constraining equations posed by the unaugmented static sub-graph. This premise is proven in Appendix A2.



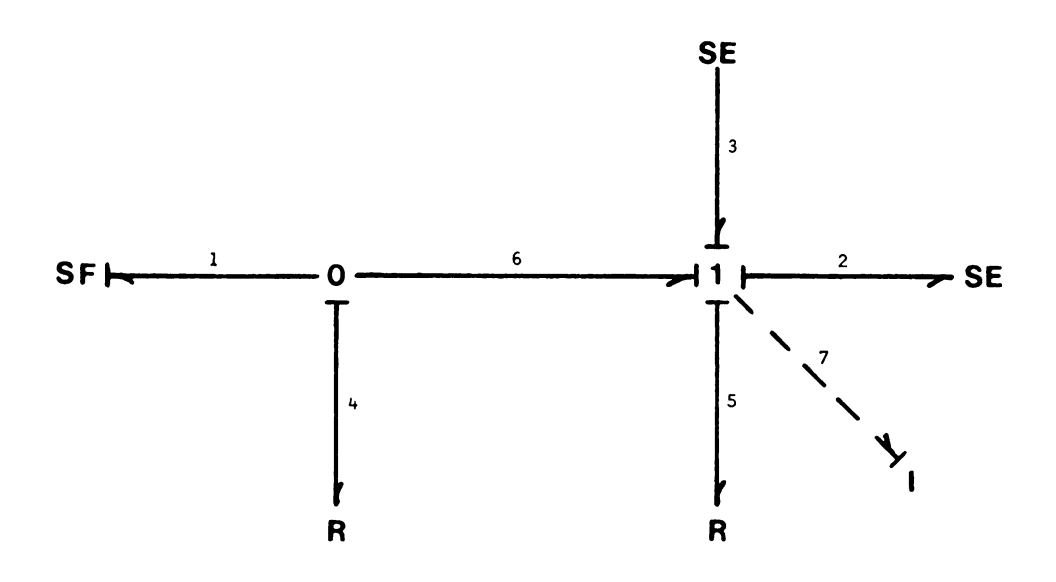


FIGURE 3-1. A DYNAMICALLY AUGMENTED SUBGRAPH



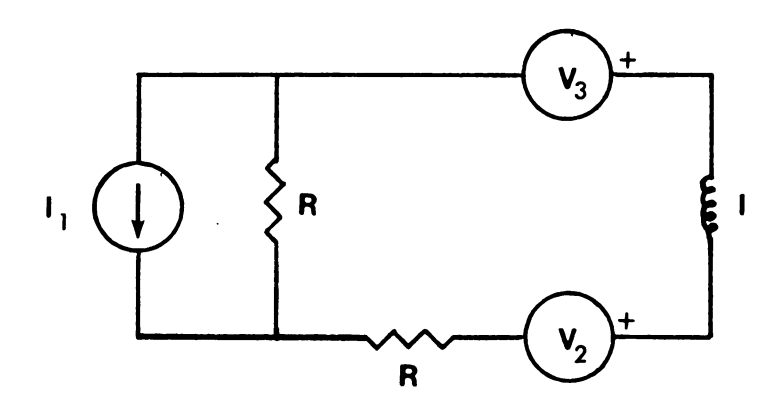


FIGURE 3-2. AN ELECTRICAL ANALOG



3.2 Minimum-Maximum Order Augmentation

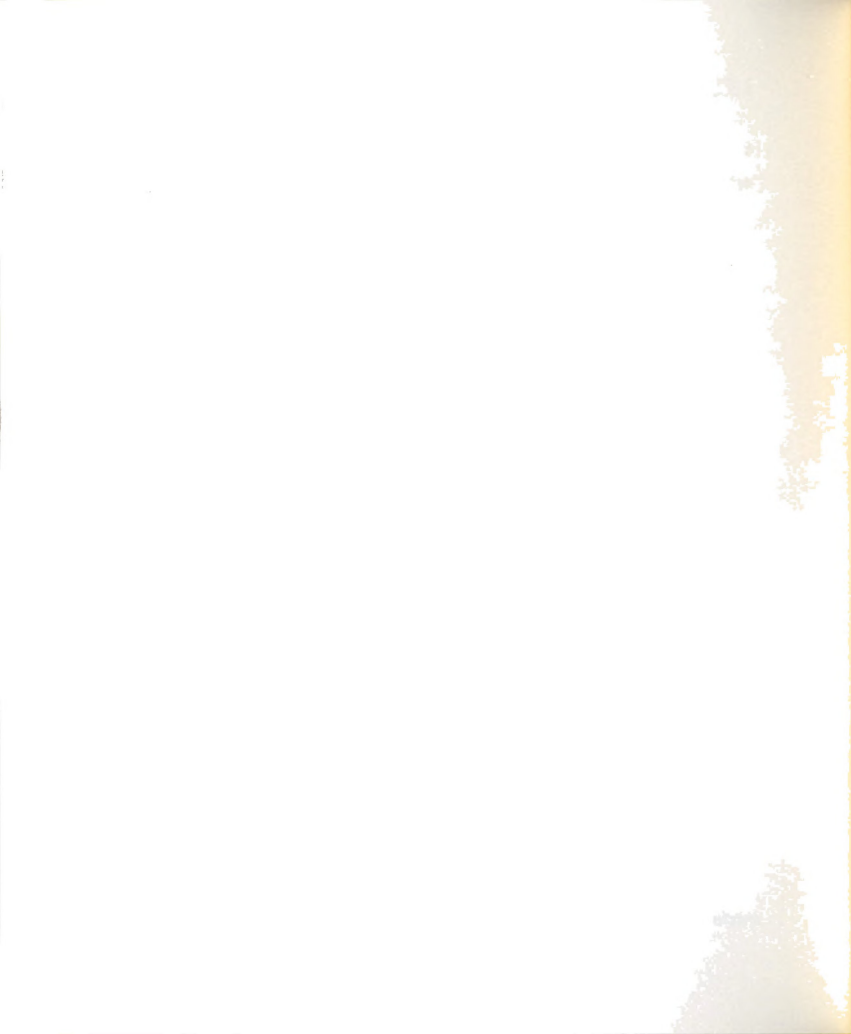
Returning to Figure 3-2, it may be inferred that three different possible augmentations exist which serve to completely extend causality. With each different augmentation a different causality orientation results on the dissipative elements. Depending on the nature of the nonlinear dissipation functions, there will exist a preferred causal orientation on the R-elements. For our example problem which had the form of the dissipative functions prescribed in equations (2-3) and (2-4), Figure 3-3 represents the desired causal arrangement with augmented C and I elements.

To the observant reader, it may be apparent that only 3 causal arrangements are realizable through selective dynamic augmentation. However, the dissipative functions may conform to four unique causal arrangments. For the fourth situation, the method of dynamic augmentation is inadequate to establish the preferred causal orientations on both dissipative elements.

From the preceding discussion, it is apparent that a structural modification using selective dynamic augmentation of a static-subgraph is not unique.

The introduction of each additional dynamic element into a sub-graph increases the dynamic order of that system. Also, associated with each dynamic element introduced is a free parameter. In general, the order of the dynamically augmented system is bounded by a minimum and maximum order augmentation.

With a minimum order augmentation, complexity is certainly checked, however, a maximum order augmentation may allow greater



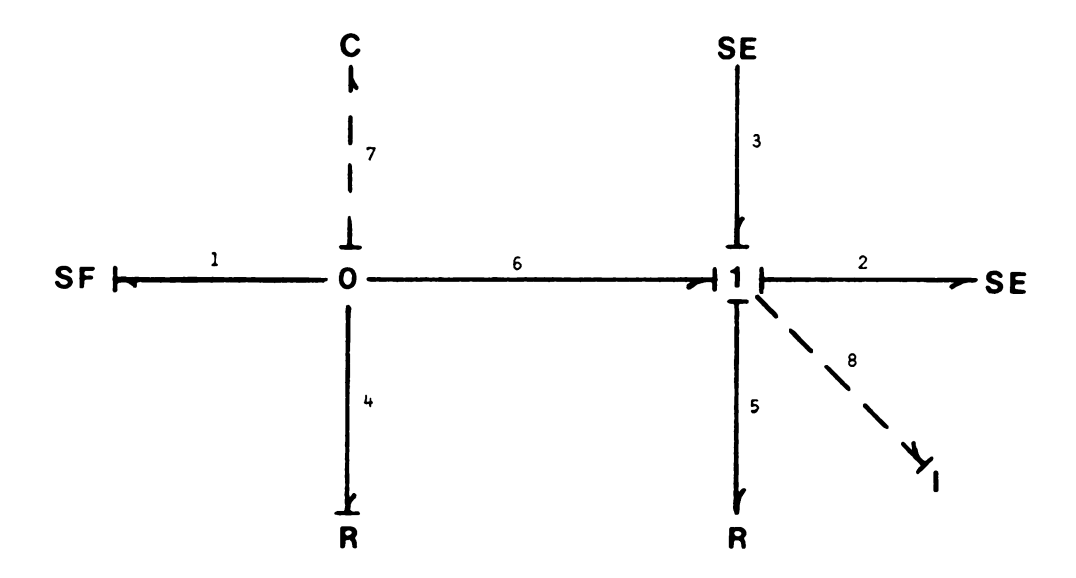


FIGURE 3-3. THE PREFERRED DYNAMIC AUGMENTATION



latitude in tailoring the augmented system's dynamics. These notions will be discussed in further detail in the ensuing section.

3.2.1 Example 2

In Figure 3-4, an analogous electrical and mechanical system with its bond-graph is shown. Again, this bond-graph exhibits an acausal fragment associated with a dissipative field. The diagnosis was rendered following the standard causal augmentation procedure [1].

Figure 3-5 shows the seven available dynamic augmentations to completely extend the causality in the sub-graph. The minimum order augmentation (2nd order) for this particular sub-graph, is pictured in Figure 3-5a, d, the maximum order (4th order) is shown in Figure 3-5g. The selection of a particular augmentation scheme would be influenced by the implied causal nature of the nonlinear dissipation functions in the field.

3.3 The Secondary Dynamics Problem

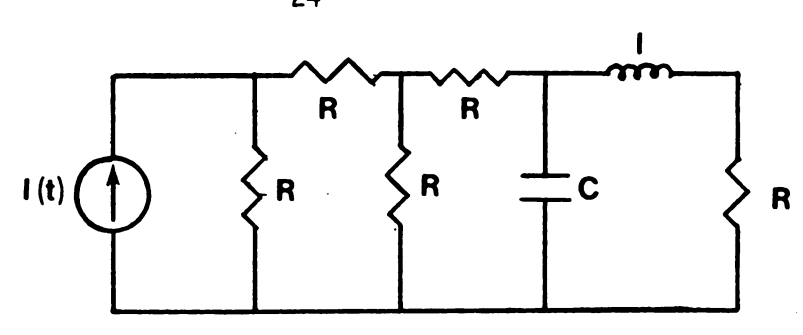
3.3.1 Linear Dissipative Fields

For the dynamically augmented sub-graph, the system representation is readily resolved into an explicit state-space form.

$$\dot{x} = Ax + Bu \tag{3-1}$$

Structurally, the A matrix reveals the following form:

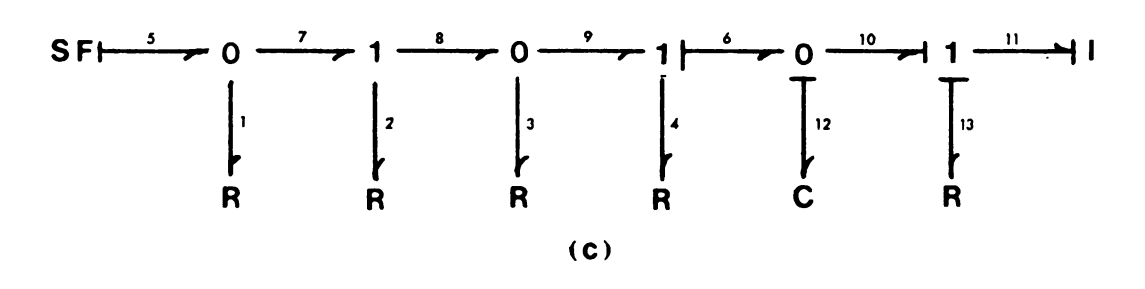




(a)



(b)



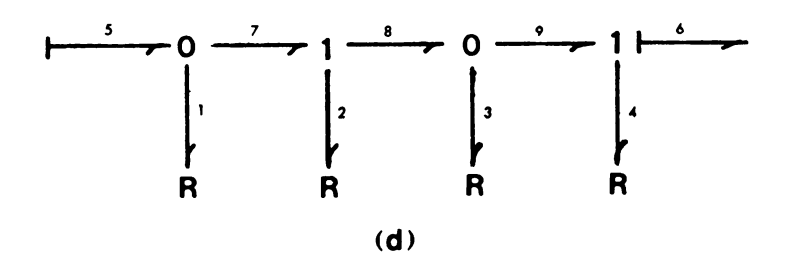


FIGURE 3-4. A BOND GRAPH EXAMPLE

- a) ELECTRIC CIRCUIT
- b) MECHANICAL SYSTEM
- c) THE BOND GRAPH MODEL
- d) THE ACAUSAL SUBGRAPH



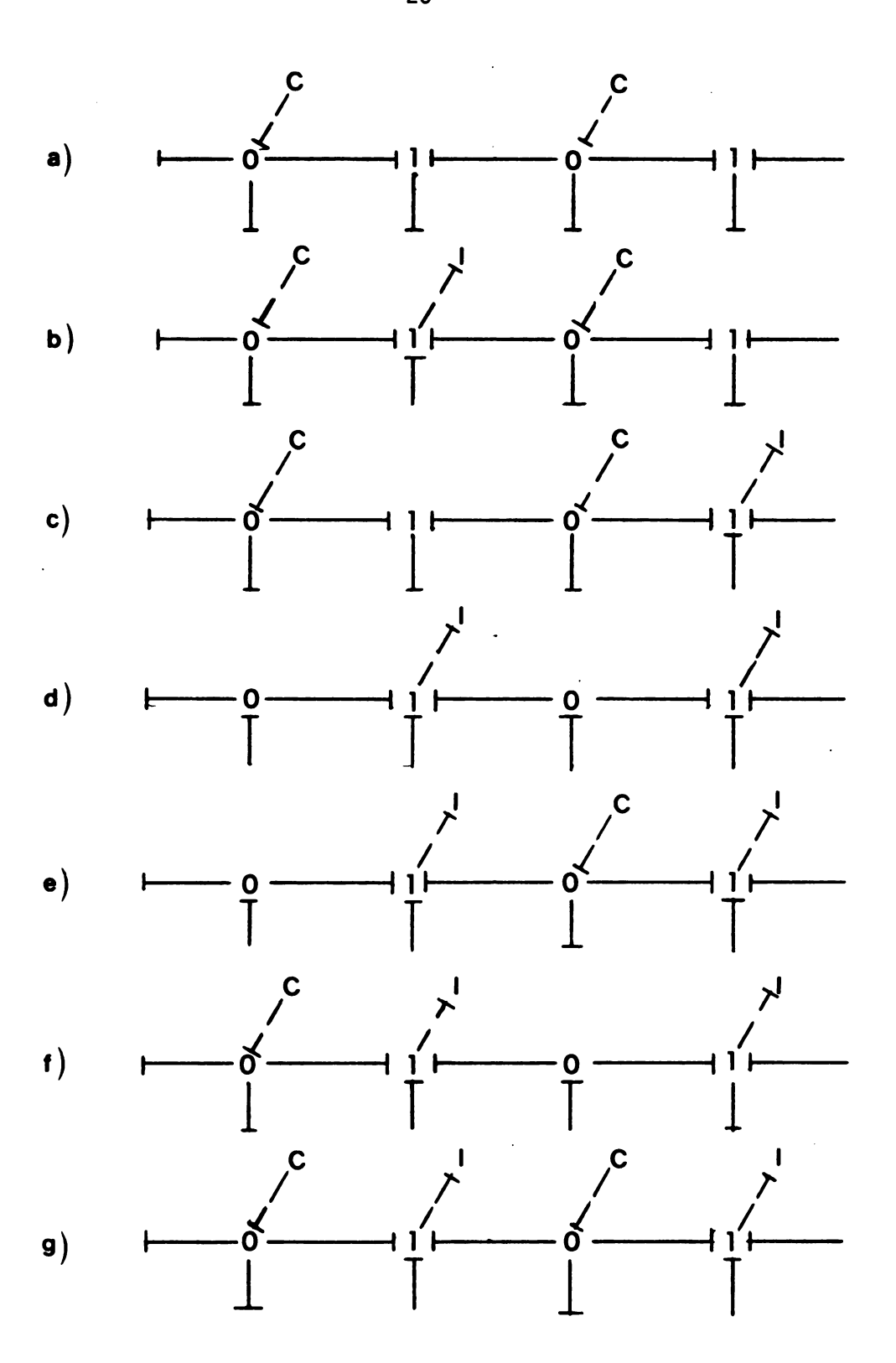
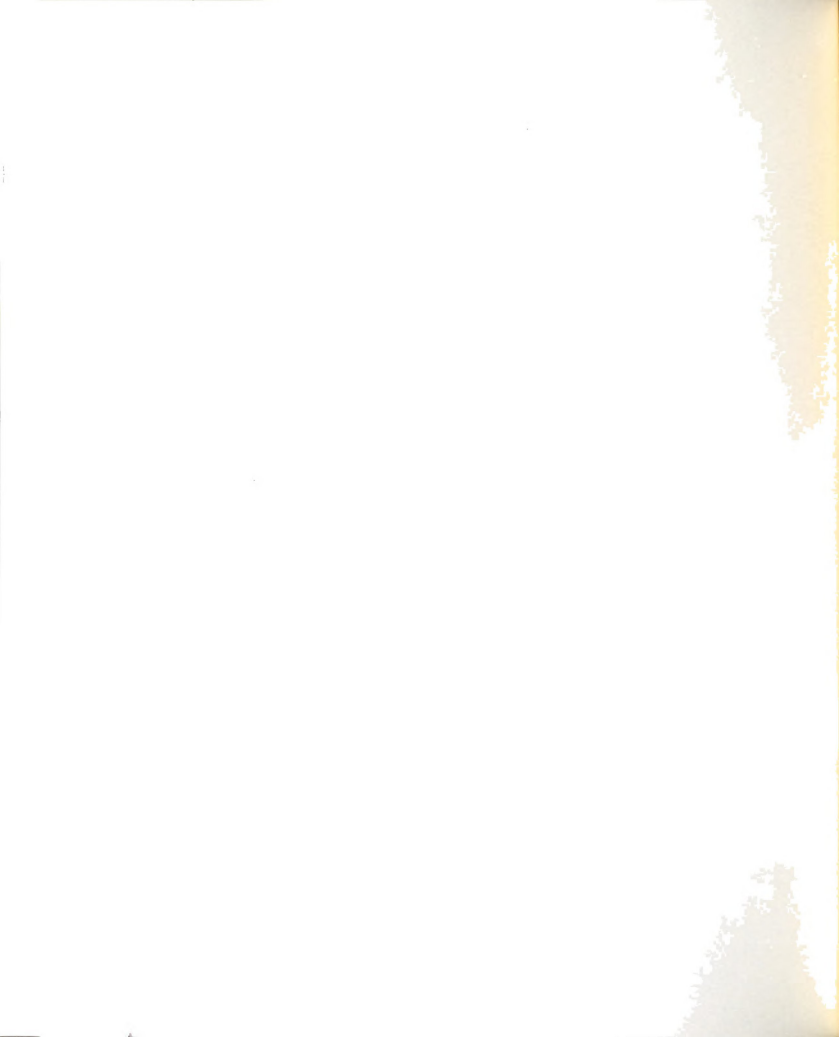


FIGURE 3-5. POSSIBLE DYNAMIC AUGMENTATIONS



$$A = - \begin{bmatrix} s \end{bmatrix} \begin{bmatrix} \kappa \end{bmatrix}$$
 (3-2)

The S matrix is derived from the bond-graph topology and dissipation elements while the diagonal K matrix consists of the free parameters introduced through the dynamic augmentation. Confining our attention to conservative energy storage fields, it can be noted that the K-matrix will be positive definite. Also, due to the nature of the dynamically augmented subgraph, the S matrix will be, in virtually all cases, positive definite.* The input vector \mathbf{u} will be a constant vector. From the preceding statements, it follows that the linear system will be bounded output stable regardless of parameter selection (provided $\mathbf{k_i} > 0$).

Having chosen a dynamic augmentation for the 'loop' sub-graph, the remaining task is to determine a computation scheme to efficiently calculate the steady-state output vector of 'loop' subsystem. One must keep in mind that for each global time step, the steady-state output vectors of the loop sub-graphs (G_S) need to be computed.

The solution for the steady-state vector in the case of linear dissipative fields can be achieved by simple linear algebra provided the A matrix is nonsingular.

^{*}In some special cases, the S matrix may be only positive semidefinite.



$$\hat{\mathbf{x}} = \mathbf{A}^{-1} \mathbf{B} \mathbf{u} \tag{3-3}$$

Another approach to this problem consists of the dynamic simulation of the 'loop' sub-system. This concept will be particularly useful in the case of nonlinear dissipative fields. For this approach, the resulting design problem can be posed as:

How can the free parameters be selected to provide computationally efficient convergence to the steady-state output vector?

By properly selecting the free parameters, the eigenvalues may be clustered. Using the available integration scheme for the global simulation, a local integration of the 'loop' subsystem to steady state may be performed. Assuming the spectrum is compact, an optimal integration time step may be chosen relative to the entire spectrum. Hence, a minimum number of iterations would be required to converge to steady-state.

In a first order system, the selection of an optimal free parameter is simplified since any positive real constant will suffice provided the resulting system is stable. The integration time step would be chosen accordingly. Thereby, an efficient solution would be realized.

The characteristic polynomial is a useful tool for investigating the relationship of the free parameters to the eigenvalues of the 2nd order system.



Recall the special form of the A matrix:

$$A = -\begin{bmatrix} s_{11} & s_{12} \\ s_{21} & s_{22} \end{bmatrix} \begin{bmatrix} k_1 & 0 \\ 0 & k_2 \end{bmatrix}$$
 (3-4)

The characteristic polynomial for the general second order system is

$$\lambda^2 - (s_{11}K_1 + s_{22}K_2)\lambda + det[SK] = 0.$$
 (3-5)

The roots are:

$$\alpha$$
, $\beta = \frac{s_{11}K_1 + s_{22}K_2 + \sqrt{(s_{11}K_1 + s_{22}K_2)^2 - 4 \det[SK]}}{2}$ (3-6)

For repeated roots to exist,

$$\sqrt{(s_{11}K_1 + s_{22}K_2)^2 - 4 \det[SK]} = 0.$$
 (3-7)

Squaring equation (3-7) yields a 2nd degree quadratic. The general form of a 2nd degree quadratic equation is 1

$$ax^2 + 2hxy + by^2 + 2gx + 2fy + c = 0.$$
 (3-8)

The following equations define Δ and J in terms of the coefficients of equation (3-8).

¹CRC Standard Mathematical Tables.



$$\Delta \equiv \det \begin{bmatrix} a & h & g \\ h & b & f \\ g & f & c \end{bmatrix}$$
 (3-9)

$$J \equiv \begin{bmatrix} a & h \\ h & b \end{bmatrix}$$
 (3-10)

For equation (3-7), Δ =0, and J takes the form

$$J = 4s_{11}s_{22}s_{21}s_{12} - 4s_{12}^{2}s_{21}^{2}$$
 (3-11)

Considering the cases when the S matrix is positive definite, $s_{11}s_{22} > s_{12}s_{21}$. For the instances when the product $s_{12}s_{21} < 0$, the values of J is also less than zero. This fact indicates that real positive parameters k_1 and k_2 exist to effect repeated roots. For $s_{12}s_{21} > 0$, the value of J will be greater than zero. The solution of equation (3-7) will consist of complex conjugate intersecting lines. From this result, it is concluded that real positive parameters to produce repeated roots are not realizable.

Reconsider the characteristic polynomial in equation (3-5). The polynomial coefficients may be represented in terms of the roots α and β .

²CRC Standard Mathematical Tables.



$$\lambda^2 - (\alpha + \beta)\lambda + \alpha\beta = 0 \tag{3-12}$$

For the case where $s_{12}s_{21} < 0$, by setting $\alpha = \beta$ and equating coefficients in equations (3-5) and (3-12), the free parameters to effect repeated roots are determined to be

$$k_1, k_2 = \frac{\alpha}{s_{11}} \left(1 + \sqrt{1 - \frac{s_{11}s_{22}}{\det[S]}} \right)$$
 (3-13)

If the product of the off diagonal elements is greater than zero ($s_{12}s_{21} > 0$), the relationship in equation (3-14) must be satisfied to insure selection of positive real parameters. Its derivation procedes similarly to that of equation (3-13); however, α and β now represent real distinct roots.

$$\frac{\alpha}{\beta} + \frac{\beta}{\alpha} \ge \frac{4s_{11}s_{22}}{\det[S]} - 2 \tag{3-14}$$

To minimize the difference $[\alpha-\beta]$, the equality in equation (3-14) must be enforced. It is convenient to rewrite equation (3-14) as,

$$\frac{\alpha}{\beta} + \frac{\beta}{\alpha} = C; \qquad C > 2 \qquad (3-15)$$

For a given value of C, the solution pairs (α, β) form a pair of intersecting lines as shown in Figure 3-6. The slopes of these lines sum to the value of C. This result indicates that an infinity of optimal pairs (α, β) exist which are germane to our problem.



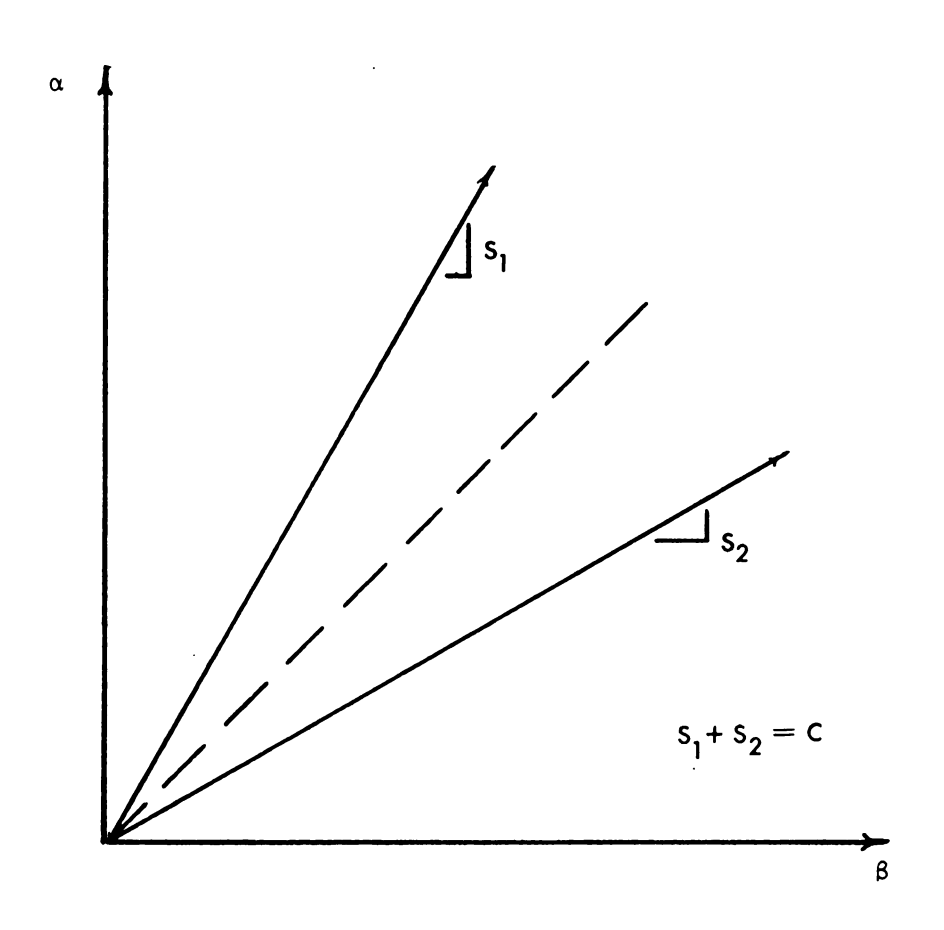


FIGURE 3-6. EIGENVALUE SEPERATION

Arbitrarily selecting α to be unity enforces the following condition on β ,

$$\frac{1}{\beta} + \frac{\beta}{1} = C \tag{3-16}$$

Equation (3-16) is predisposed to a quick iterative solution. Having specified α and β , the free parameters are determined from the following equation,

$$k_1 = \frac{\alpha + \beta}{2s_{11}} \tag{3-17}$$

$$k_2 = \frac{\alpha + \beta}{2s_{22}} \tag{3-18}$$

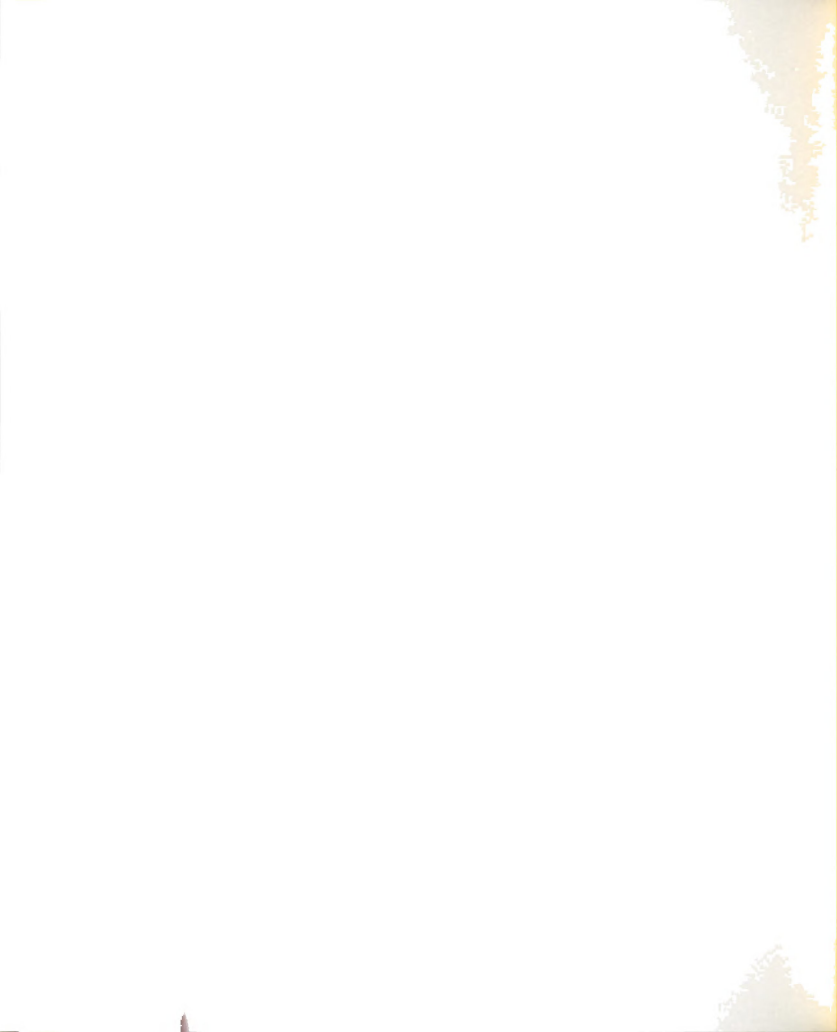
The algorithm presented in the preceding paragraphs provides a relatively efficient procedure for optimal pole placement for the class of second order systems concerned with here. Unfortunately, the utility of the method does not extend to higher order systems.

3.3.2 Nonlinear Dissipative Fields

In the case of nonlinear dissipative fields, the augmented sub-system representation takes the general form:

$$\dot{x} = \phi(x, u). \tag{3-19}$$

$$Y = \psi(x, u) \tag{3-20}$$



Again, two primary techniques are available to determine the steady state output vector $\hat{\boldsymbol{Y}}.$

The solution of equation (3-21) for \hat{x} could be accomplished by a numerical scheme such as the Newton-Raphson method.

$$0 = \phi(x, u)$$
 (3-21)

The output vector becomes readily available as

$$Y = \psi(\hat{x}, u) \tag{3-22}$$

Intrinsic difficulties in convergence and computational efficiency detract from this type of numerical method.

Again, as in the linear case, the desired steady state solution may be obtained through numerical integration of the nonlinear state equations provided the system is stable. Stability is contingent on the nature of the dissipative field. Parameter selection will play a deciding role in the stability of sub-systems comprised of certain classes of dissipative fields.

In referring to nonlinear systems, one can no longer speak of eigenvalues. A useful and often employed technique in the analysis of nonlinear systems is linearization about a nominal trajectory or singular point. The resultant eigenvalues of the linearized system will approximate the local dynamics of the nonlinear system. This technique allows the dynamicist to identify the relevant time scales in the system. This notion will be



exploited in the development of a parameter selection scheme for nonlinear systems.

To appreciate the intercoupling of the free parameters in the nonlinear problem, an example problem will be discussed.

Reconsider the physical systems in Figure 3-4. The bond graph for the analogous electrical and mechanical systems is also shown in this figure. As was indicated earlier, this bond-graph engenders an algebraic loop. The static sub-graph with possible dynamic augmentations is shown in Figure 3-5. For this example, the augmentation of Figure 3-5a has been chosen. Figure 3-7 depicts the augmented sub-graph, state vector, and dissipation functions.

With little effort, the state equations for this system can be derived from the bond-graph model. The state variables q_{10} and q_{11} represent the compliance effects and the free parameters k_1 and k_2 are represented by $1/C_{10}$ and $1/C_{11}$ for this system.

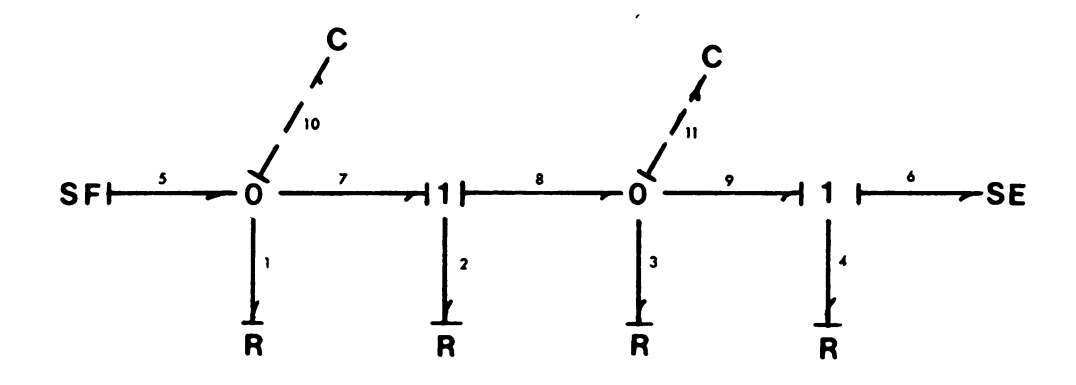
$$\dot{q}_{10} = -\phi_1 \left(\frac{q_{10}}{c_{10}}\right) -\phi_2 \left(\frac{q_{10}}{c_{10}} - \frac{q_{11}}{c_{11}}\right) + f_5$$
 (3-23)

$$\dot{q}_{11} = \phi_2 \left(\frac{q_{10}}{c_{10}} - \frac{q_{11}}{c_{11}} \right) - \phi_4 \left(\frac{q_{11}}{c_{11}} - E_6 \right) - \phi_3 \left(\frac{q_{11}}{c_{11}} \right)$$
 (3-24)

The output vector is defined as,

$$e_5 = q_{10}/c_{10}$$
 (3-25)
 $f_6 = \phi_4 (q_{11}/c_{11} - E_6)$





$$\mathbf{x} = \begin{bmatrix} \mathbf{q}_{10} \\ \mathbf{q}_{11} \end{bmatrix}$$

$$\mathbf{y} = \begin{bmatrix} \mathbf{e}_{s} \\ \mathbf{f}_{\delta} \end{bmatrix}$$

$$\mathbf{u} = \begin{bmatrix} \mathbf{f}_{5} \\ \mathbf{e}_{6} \end{bmatrix}$$

DISSIPATION FUNCTIONS

$$\mathbf{f}_1 = \phi_1 (\mathbf{e}_1)$$

$$\mathbf{f_2} = \phi_2(\mathbf{e_2})$$

$$f_3 = \phi_3 (e_3)$$

$$f_4 = \phi_4 (e_4)$$

$$f_4 = \phi_4 \left(\mathbf{e}_4 \right)$$

FIGURE 3-7. AN AUGMENTED SUBGRAPH



Suppose the dissipative functions are specified as follows:

$$f_1 = e_1^3$$
 $f_2 = e_2^2$
 $f_3 = e_3$
 $f_4 = e_4^5$
(3-26)

The linearized A matrix of this particular system about the hypothetical equilibrium point \hat{q}_{10} , \hat{q}_{11} yields,

$$A = \begin{bmatrix} (\frac{-3\hat{q}_{10}^{2}}{c_{10}^{3}} - \frac{2\hat{q}_{10}}{c_{10}^{2}} + \frac{2\hat{q}_{11}}{c_{10}c_{11}}) & 2(\frac{\hat{q}_{10}}{c_{10}c_{11}} - \frac{\hat{q}_{11}}{c_{11}^{2}}) \\ 2(\frac{\hat{q}_{10}}{c_{10}^{2}} - \frac{\hat{q}_{11}}{c_{10}c_{11}}) & -2(\frac{\hat{q}_{10}}{c_{10}c_{11}} - \frac{\hat{q}_{11}}{c_{11}^{2}}) - \frac{5}{c_{11}}(\frac{\hat{q}_{11}}{c_{11}} - E_{6})^{4} - \frac{1}{c_{11}} \end{bmatrix}$$

$$(3-27)$$

As conveyed by the complicated form of the A matrix in equation (3-27), the free parameters play a nontrivial role in the adjustment of the timescales in the nonlinear problem.

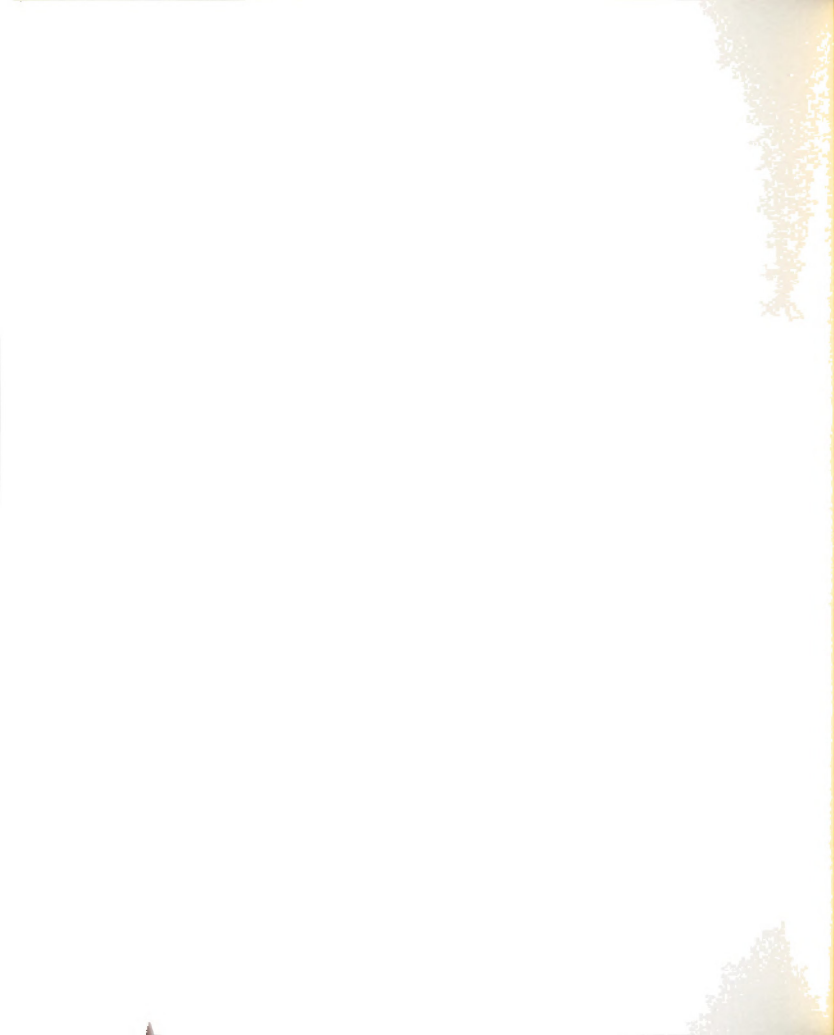
In Table 3-1, and in Figures 3-8 through 3-13, the dynamic response of the example system described earlier in Figure 3-4 and equations (3-23) through (3-26) is studied for various conditions. The example problem is useful in illustrating several properties exhibited by the class of nonlinear systems associated with the dynamic augmentation of dissipative fields.

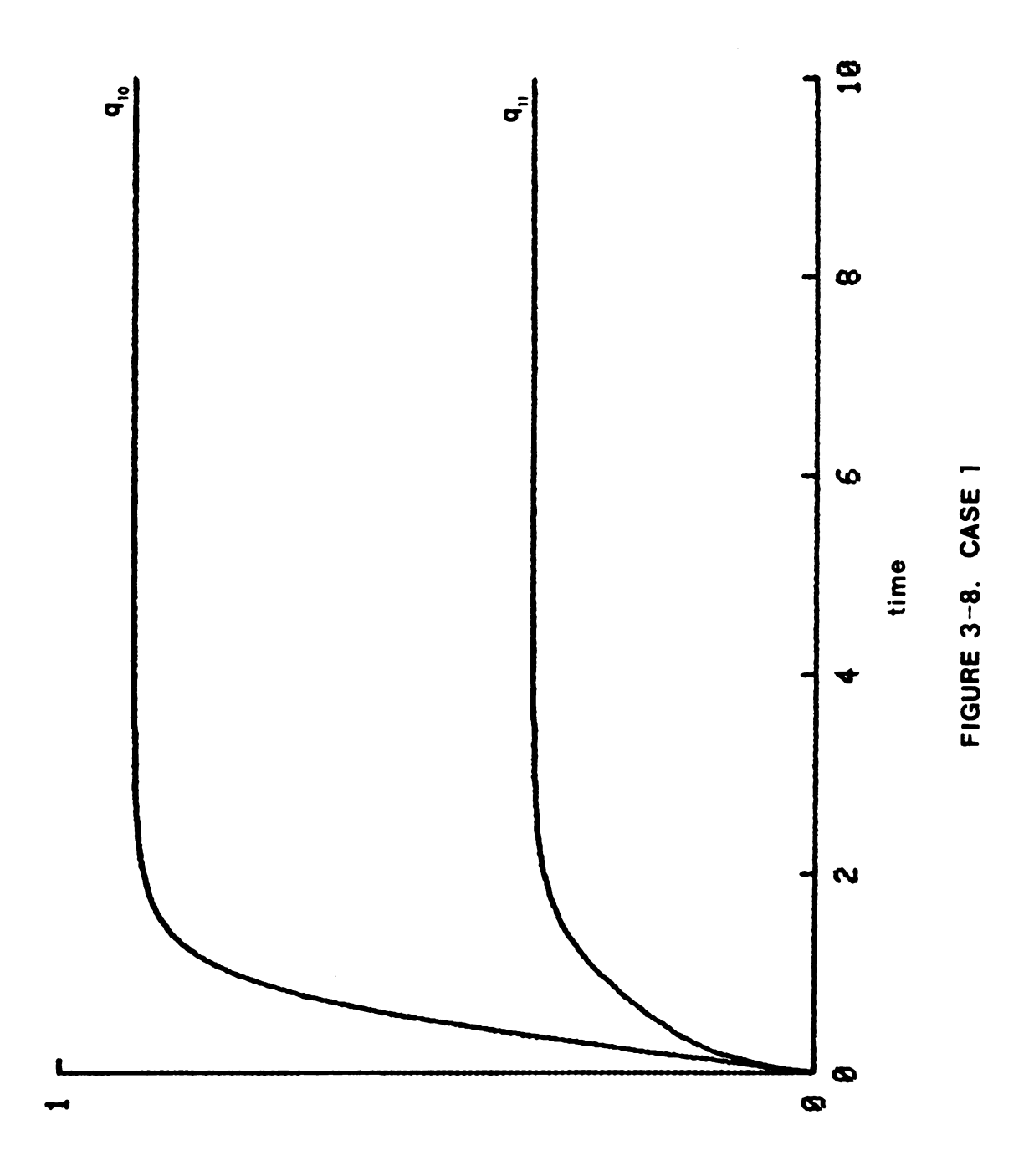


TABLE 3-1 Simulation Data

	Input	Input Vector	Free Paramet	rameters*	Derivati	Derivative Vector	State Vector	/ector	Output Vector	Vector	Comments
Case	F5	E6	۸ _		أ ₁₀	٩٦٦	9 ₁₀	qıı	E5	F6	
L #	1.0	1.0	1.0	1.0	000.0	000.0	.8980	.3729	.8980	0260	
#2	1.0	1.0	.20	2.0	0.000	0.000	4.49	.1864	.8980	0970	
#3	1.0	1.0	1.16	.52	000.0	0.000	.7742 .7170	.7170	.8980	0.0970	Optimal Parameters
#4	.2	9.	1.0	1.0	000.0	0.000	.4547 .1291	.1291	.4547	0231	
45	.2	9.	1.25	.67	000.0	0.000	.3638 .1937	.1937	.4547	0231	
9#	1.0	1.0	.000	100.			Unstable	a)			Parameter Induced Instability

 $*k_1 = 1/c_{10}; k_2 = 1/c_{11}.$







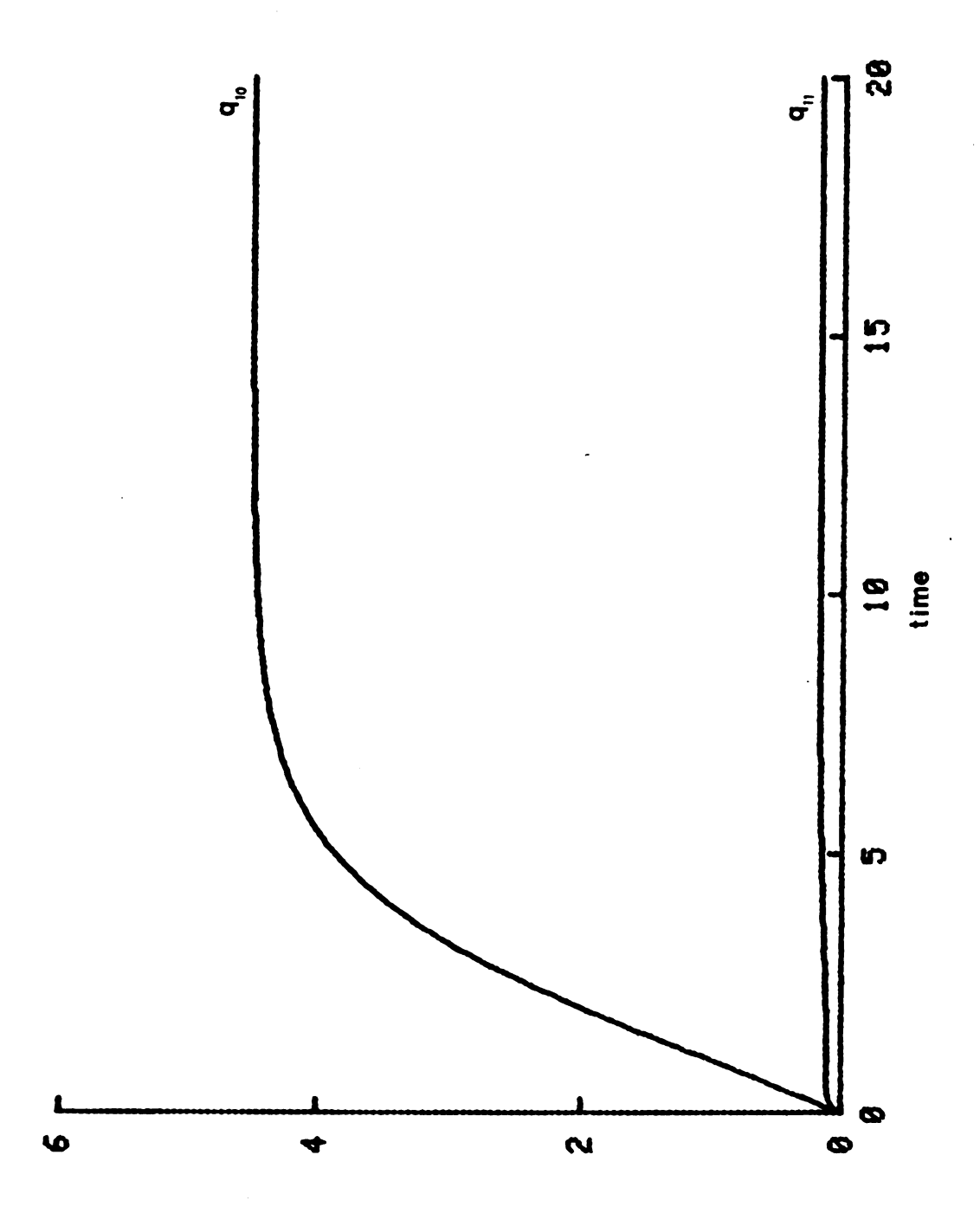
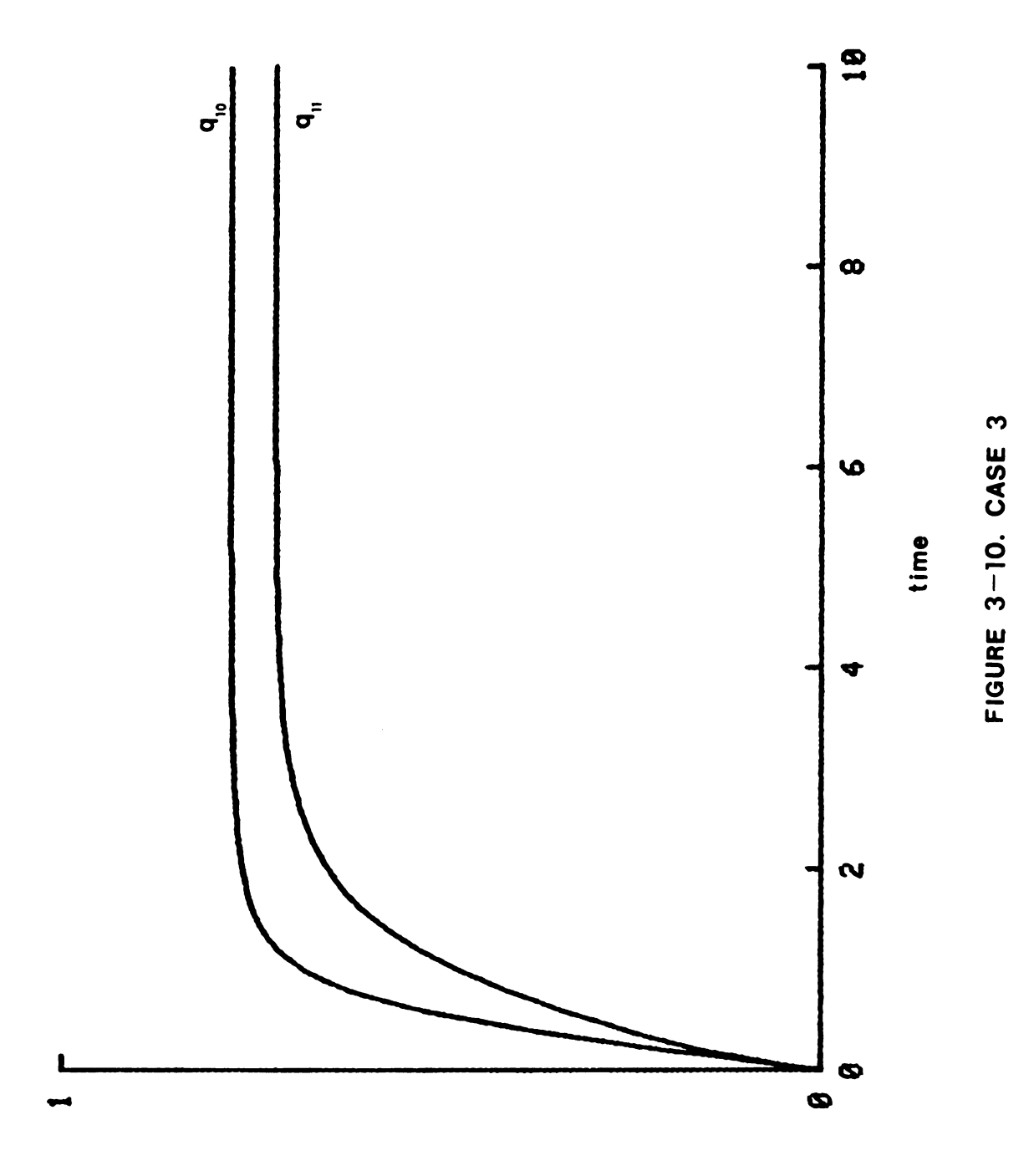
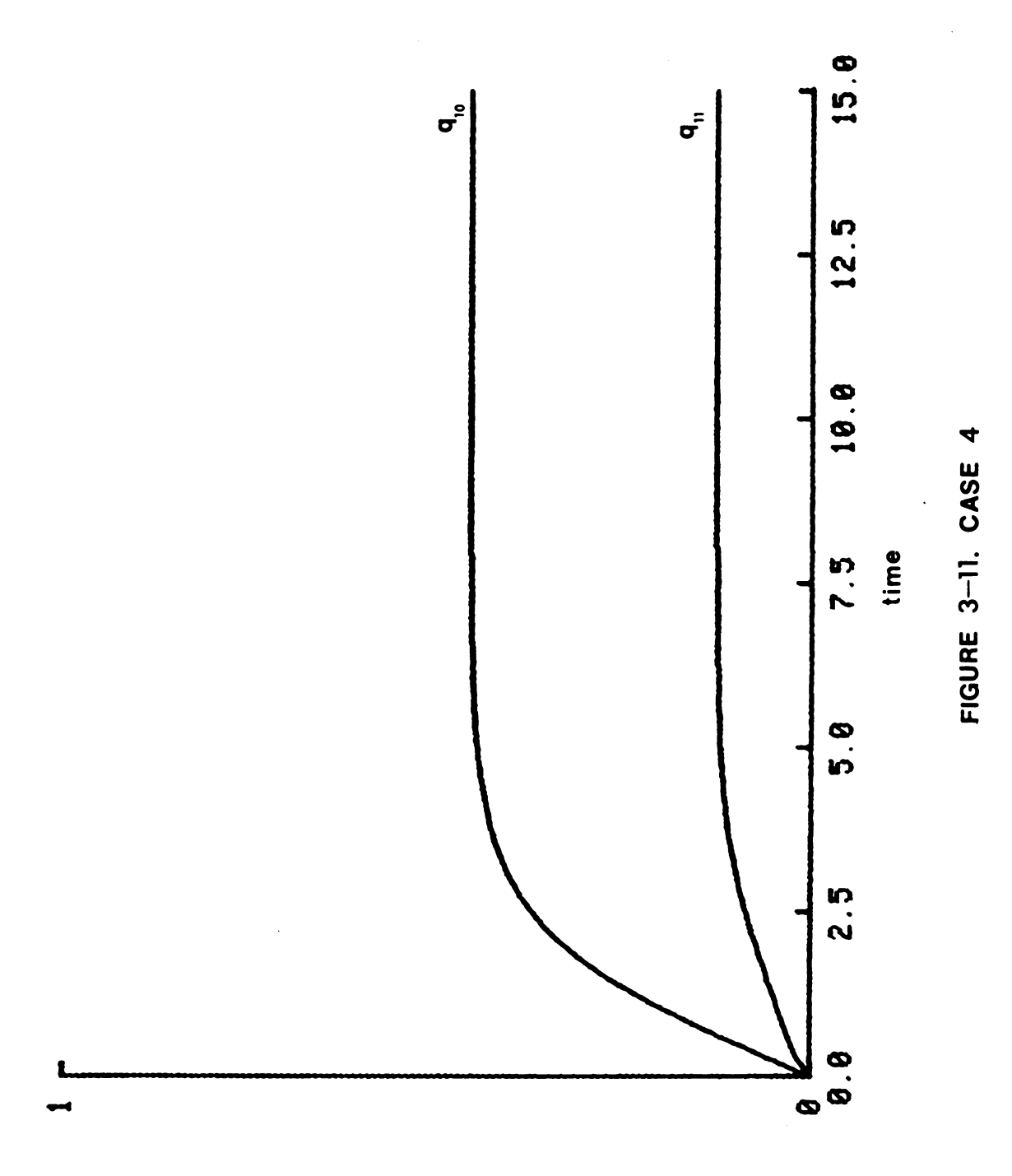


FIGURE 3-9. CASE 2









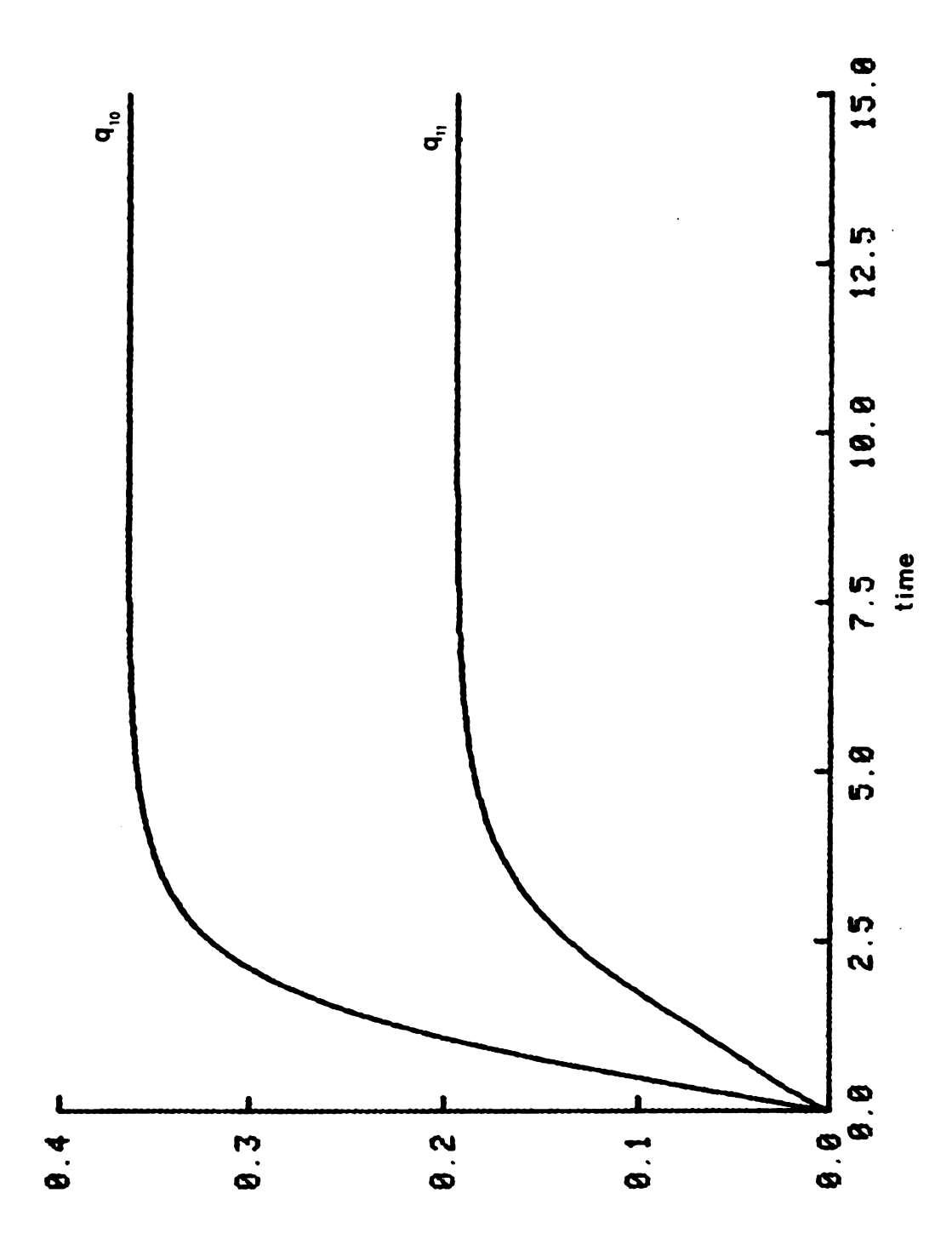


FIGURE 3-12, CASE 5



For cases 1, 2, and 3 listed in Table 3-1, the input vector remains the same, but the free parameters pairs are changed. As is evident from the data in Table 3-1, the steady-state output vector remains immutable regardless of the parameter selection (provided they are positive). Comparison of Figures 3-8 and 3-9 demonstrate the effect of parameter selection on the spreading of the time scales in the system. In case 4 and case 5, the input vector has been redefined producing a new steady-state output vector. In case 6, instability has been induced through adverse parameter placement.

3.3.3 Parameter Selection in the Nonlinear Problem

Clearly, the previous example reveals the interplay of the free parameters in the modulation of the timescales for the dynamics problem. A simple and efficient method to select the free parameters for the nonlinear problem remains to be addressed.

The following technique suggests a method of recasting the task of parameter selection for the nonlinear problem into an equivalent linear problem.

Recall that during the simulation of an entire system, the steady-state output vectors of the augmented sub-systems are required at each global time step. At each call for the steady state output vector of an augmented sub-graph (G_S) , the state of the entire system is available from the previous time step. Therefore, the instantaneous values of the effort and flow bond variables for the entire bond-graph model have been determined.

Digressing for a moment, reconsider the bond-graph model in Figure 3-4. If this system consisted of strictly linear dissipative elements, the explicit state-space form derived from the bond-graph is,

$$\begin{bmatrix} \dot{q}_{10} \\ \dot{q}_{11} \end{bmatrix} = - \begin{bmatrix} (\frac{1}{R_1} + \frac{1}{R_2}) & -\frac{1}{R_2} \\ -\frac{1}{R_2} & (\frac{1}{R_2} + \frac{1}{R_3} + \frac{1}{R_4}) \end{bmatrix} \begin{bmatrix} \frac{1}{C_{10}} & 0 \\ 0 & \frac{1}{C_{11}} \end{bmatrix} \begin{bmatrix} q_{10} \\ q_{11} \end{bmatrix} + \begin{bmatrix} F_5 \\ \frac{E_6}{R_4} \end{bmatrix}$$
(3-28)

The assumed form for the linear dissipative functions used in deriving equation (3-28) is

$$e = Rf (3-29)$$

Using the instantaneous values for the bond variables available from the previous time step, an instantaneous equivalent linear resistance 'R' can be computed for each disspative element by employing equation (3-29).

With the equivalent linear resistances, an estimate of the instantaneous dynamics of the nonlinear system can be obtained by the extraction of the eigenvalues from the A-matrix of equation (3-30) rewritten below.

$$A = -\begin{bmatrix} (\frac{1}{R_1} + \frac{1}{R_2}) & -\frac{1}{R_2} \\ -\frac{1}{R_2} & (\frac{1}{R_2} + \frac{1}{R_3} + \frac{1}{R_4}) \end{bmatrix} \begin{bmatrix} \frac{1}{C_{10}} & 0 \\ 0 & \frac{1}{C_{11}} \end{bmatrix}$$
(3-30)

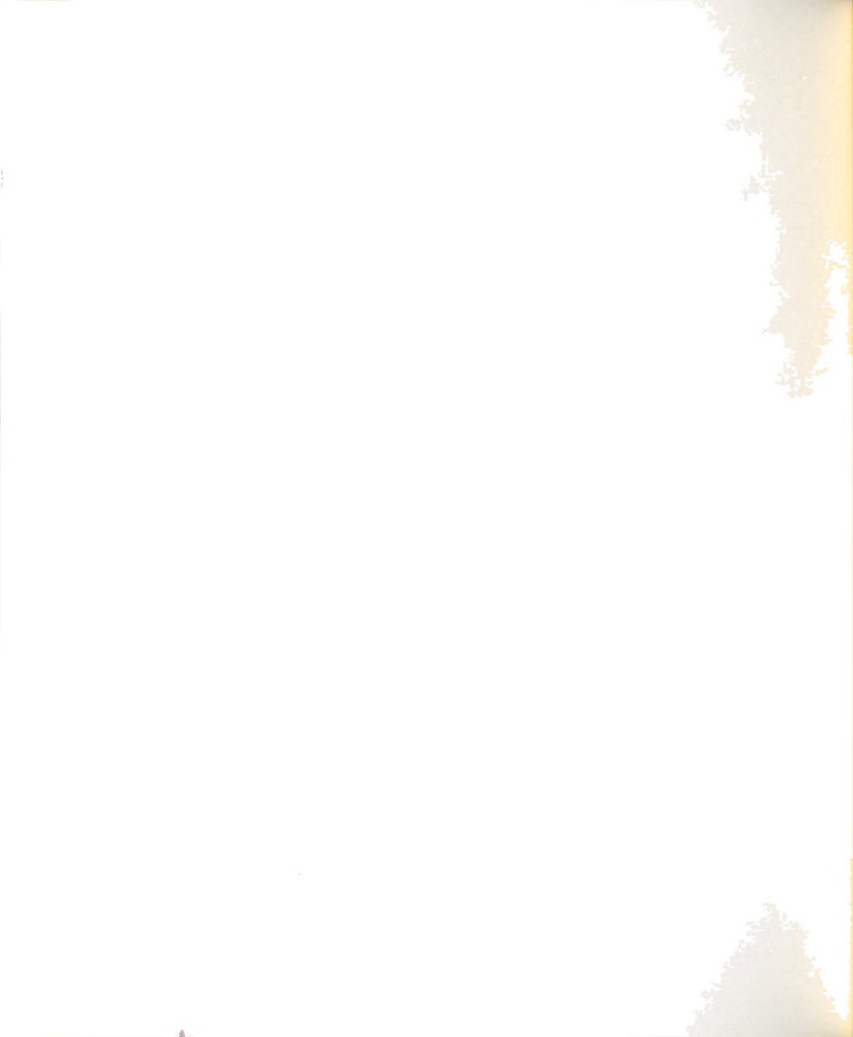


This form of the A-matrix is exactly analogous to the form presented in Section 3.3.1 for linear systems. For this form, optimal pole placement can be effected by reselection of C_{10} and C_{11} employing the method for 2nd order systems developed earlier.

The process described in the preceding paragraphs can be repeated as the global time variable increments; that is, the free parameters could be reselected intermittently throughout the global simulation in a prescribed fashion.

The technique of parameter selection for the 2nd order nonlinear problem is summarized below.

- 1) At t = t_0 , set all free parameters to unity. Compute the state of the R field. Integrate the entire system to t_0 + Δt .
- 2) Compute the instantaneous equivalent linear resistances for each nonlinear dissipative element in the augmented sub-graphs.
- 3) Compute the A matrices for the analogous linear systems.
- 4) Select optimal free parameters.
- 5) Compute the steady-state output vectors of the augmented sub-graphs.



- 6) Continue with the global integration.
- 7) Repeat the parameter selection process following a prescribed number of elapsed time steps.

To effect the most efficient convergence to steady-state for the subsequent integrations of the augmented subgraph, the initial conditions for the augmented sub-graphs should be updated using the previously computed steady-state variables,

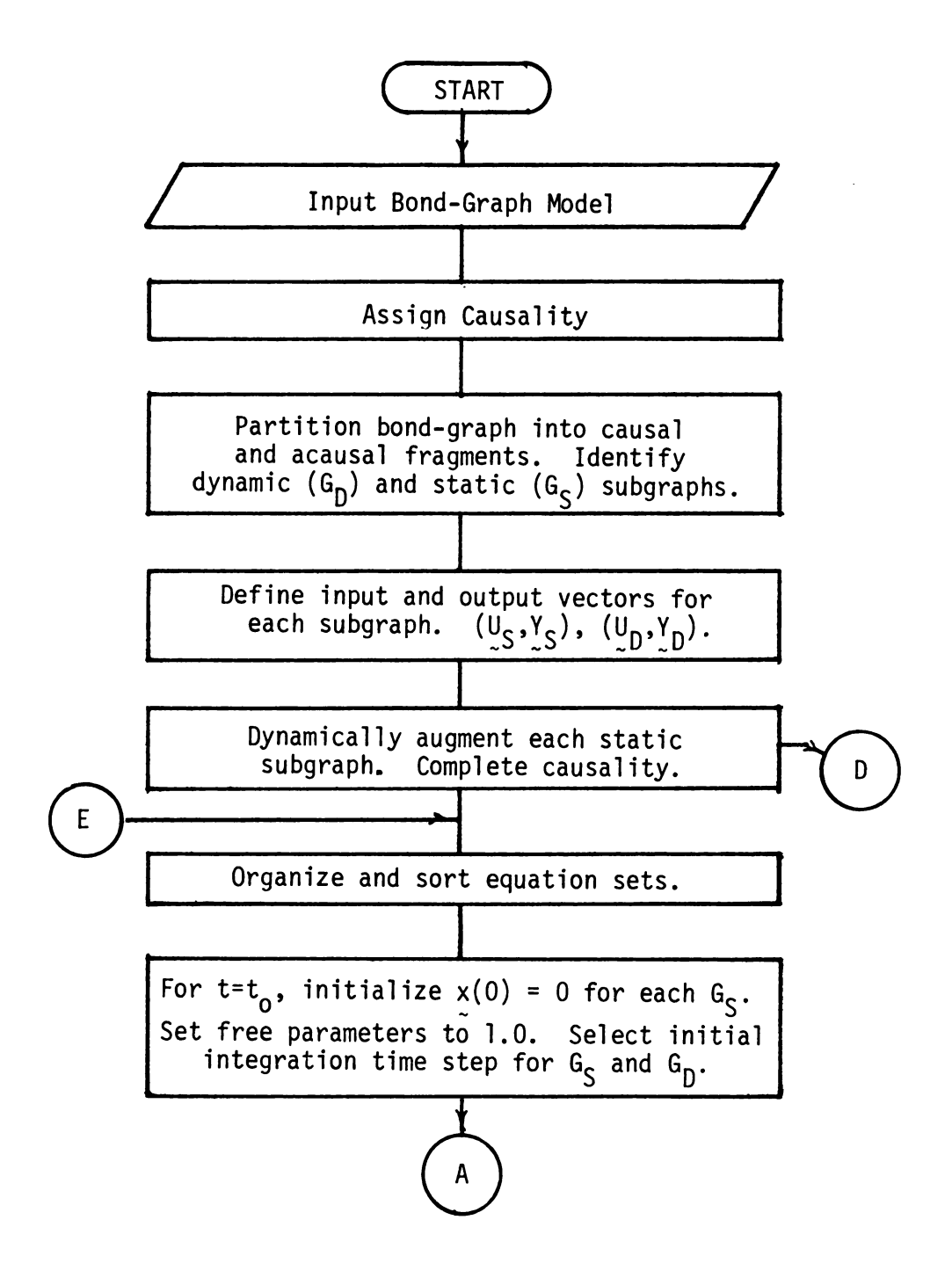
$$x_{t_d}(0) = \frac{\hat{x}_{t_{d-1}}}{k_{t_{d \text{ opt.}}}}$$
 (3-31)

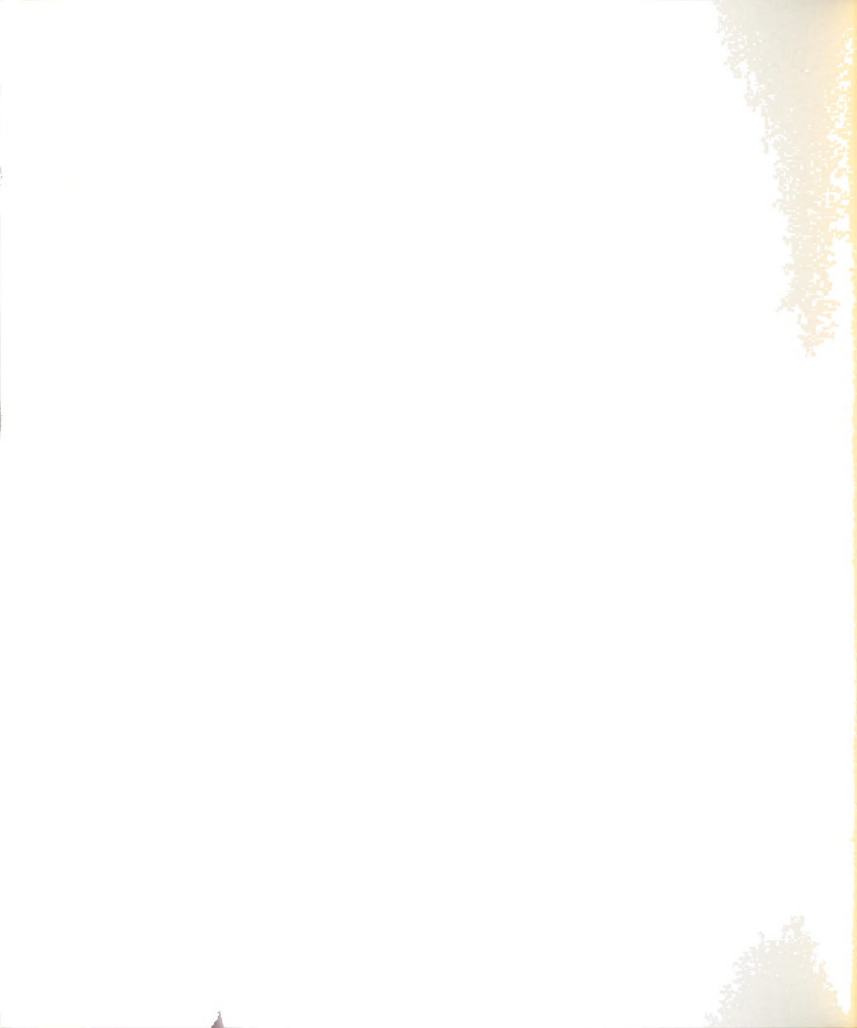
This ploy substantially decreases computational expenditure when used for each sub-graph integration call.

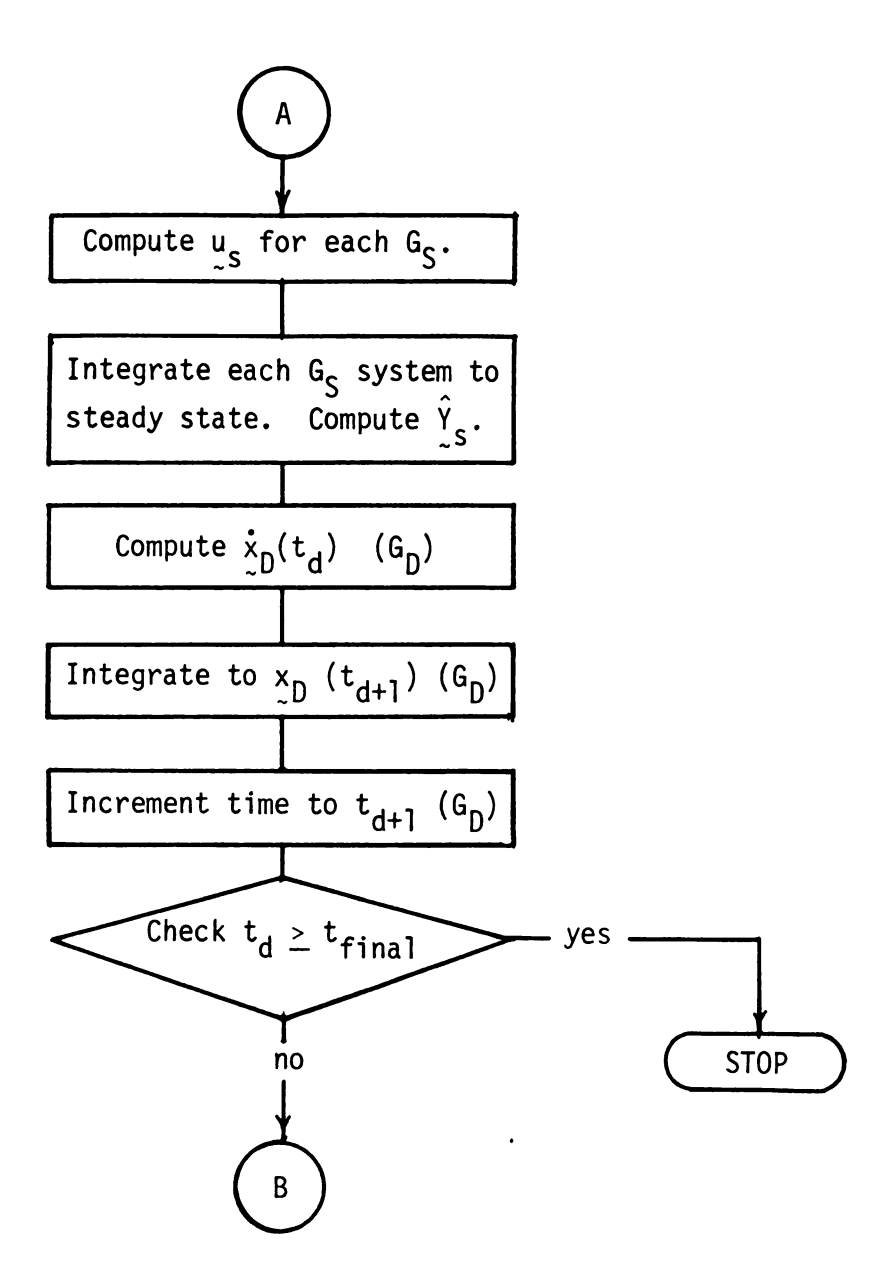
3.4 The Solution Flowchart

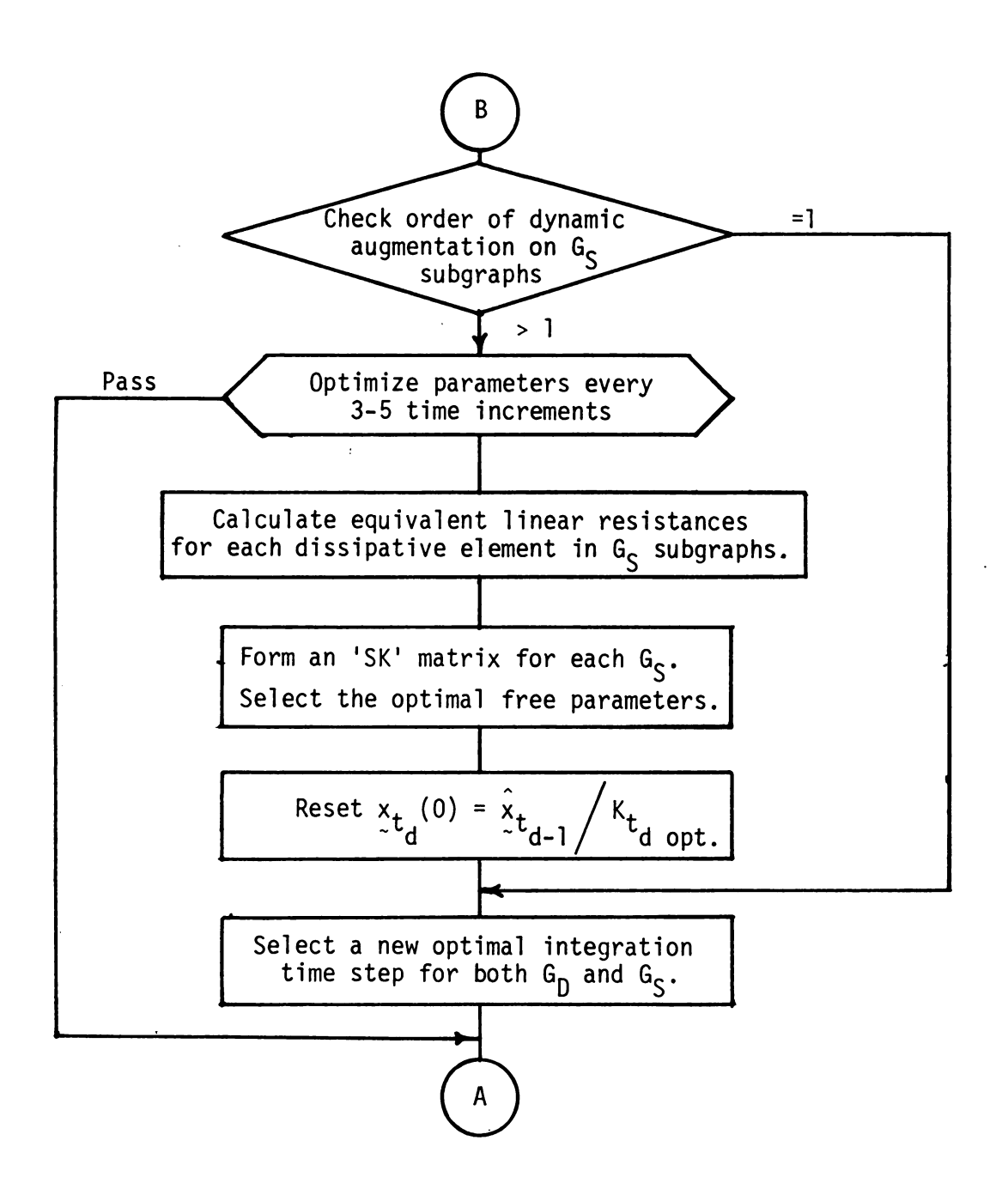
To facilitate the understanding of the solution process as it pertains to a bond-graph model containing algebraic loops, the following pages delineate the logistical hierarchy in flow-chart form. In Figure 3-14, the solution process described in the logic diagram is illustrated.

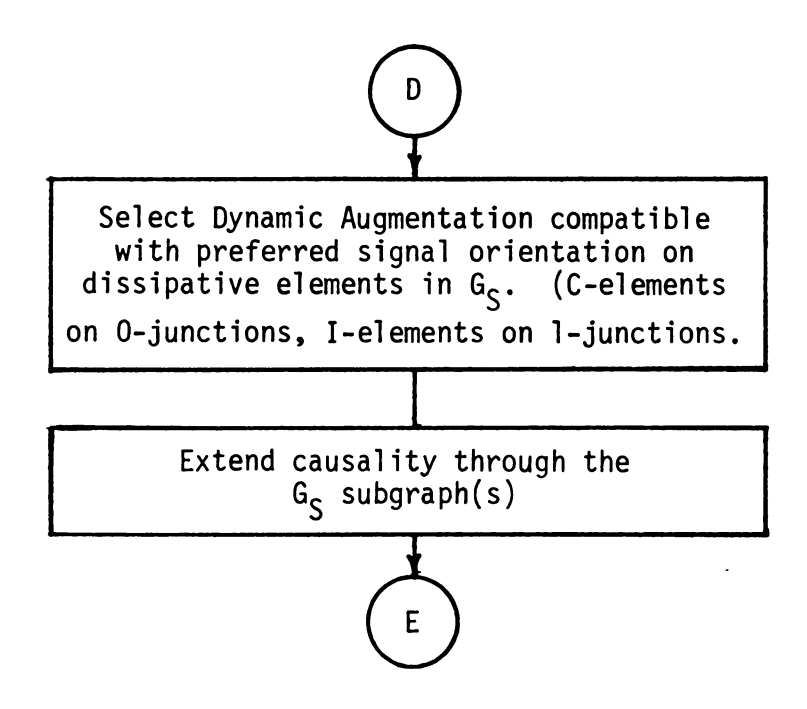
The subsequent chapter contains several examples of the implementation of the parameter selection process for nonlinear dynamically augmented sub-systems.













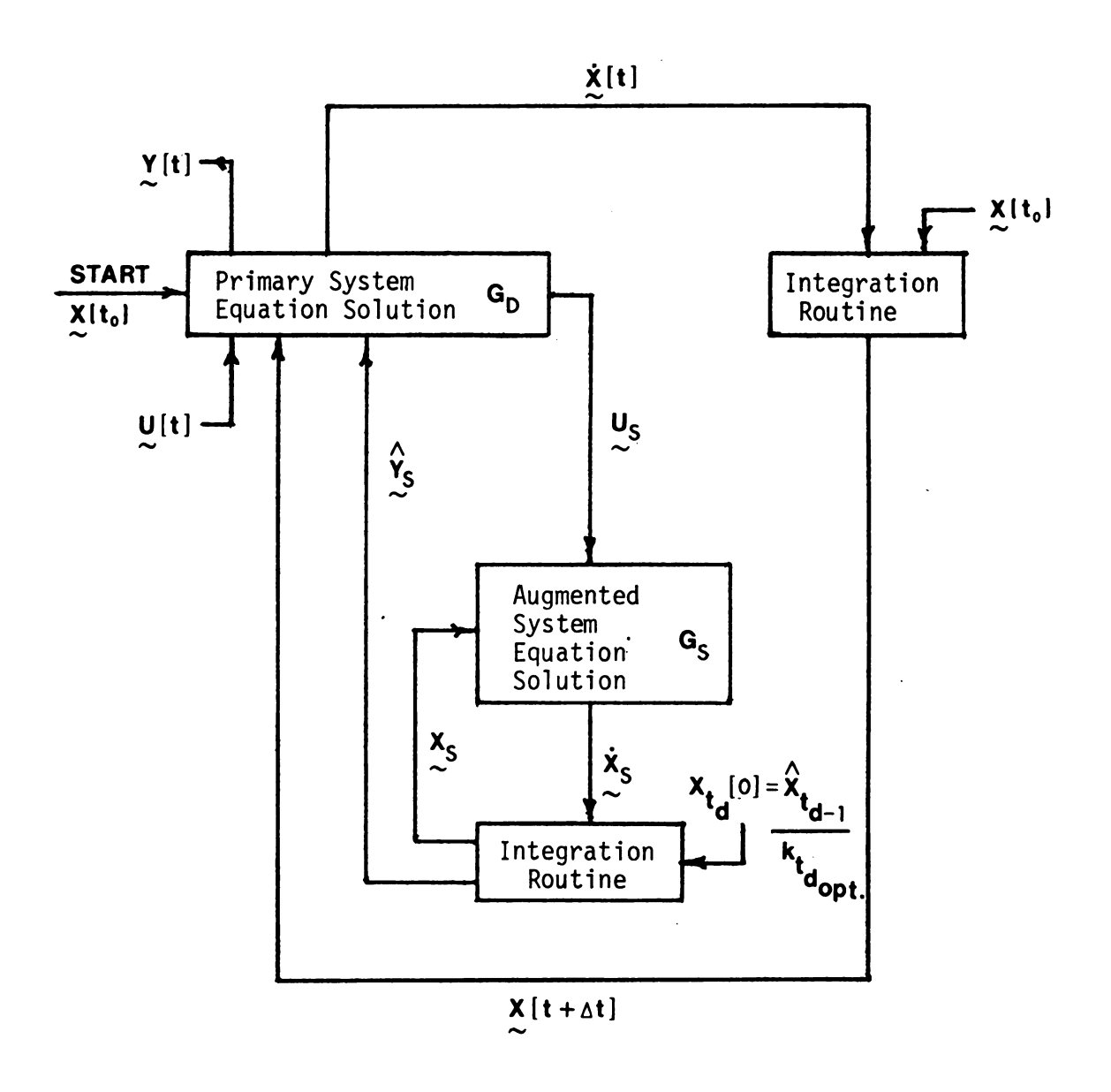


FIGURE 3-13. SOLUTION PROCESS DIAGRAM

4.0 NUMERICAL EXAMPLES

4.1 Example 1

Returning to the augmented sub-system in Figure 3-4, the explicit nonlinear state space form was found to be

$$\begin{bmatrix} \dot{q}_{10} \\ \dot{q}_{11} \end{bmatrix} = \begin{bmatrix} -(\frac{q_{10}}{C_{10}})^3 - (\frac{q_{10}}{C_{10}} - \frac{q_{11}}{C_{11}})^2 + F_5 \\ (\frac{q_{10}}{C_{10}} - \frac{q_{11}}{C_{11}})^2 - (\frac{q_{11}}{C_{11}}) - (\frac{q_{11}}{C_{11}} - E_6)^5 \end{bmatrix}$$
(4-1)

Suppose the input vector is defined at \mathbf{t}_{o} in the global system simulation as:

$$\begin{bmatrix} F_5 \\ E_6 \end{bmatrix} = \begin{bmatrix} 1.0 \\ 1.0 \end{bmatrix} \tag{4-2}$$

Following the procedure outlined in section 3.3.3, initially the free parameters default to unity. That is,

$$\begin{bmatrix} c_{10} \\ c_{11} \end{bmatrix} = \begin{bmatrix} 1.0 \\ 1.0 \end{bmatrix}$$

The resulting steady-state output vector is computed to be



$$\begin{bmatrix} \mathsf{E}_5 \\ \mathsf{F}_6 \end{bmatrix} = \begin{bmatrix} .8980 \\ -.0970 \end{bmatrix} \tag{4-3}$$

Computing the instantaneous linear resistances yields

$$R_1 = E_1/F_1 = 1.24$$
 $R_2 = E_2/F_2 = 1.9$
 $R_3 = E_3/F_3 = 1.0$
 $R_4 = E_4/F_4 = 6.46$

(4-4)

From equation (4-5), the eigenvalues for the instantaneous linear equivalent system may be readily calculated.

$$A = -\begin{bmatrix} (\frac{1}{R_1} + \frac{1}{R_2}) & -\frac{1}{R_2} \\ -\frac{1}{R_2} & (\frac{1}{R_2} + \frac{1}{R_3} + \frac{1}{R_4}) \end{bmatrix}$$
(4-5)

$$A = \begin{bmatrix} -1.333 & .526 \\ .526 & -1.68 \end{bmatrix}$$
 (4-6)

The resultant eigenvalues for the A matrix in equation (4-6) are $\lambda_1 = -2.062$, $\lambda_2 = -.9505$. λ_1 and λ_2 indicate the relative timescales of the system response for the parameters set to 1.0. Figure 4-1 illustrates the response of the system for this case.

The input vector from \mathbf{G}_{D} to the sub-system \mathbf{G}_{S} will be updated at the subsequent global time step. Suppose its updated value is

$$\begin{bmatrix} F_5 \\ E_6 \end{bmatrix} = \begin{bmatrix} 1.2 \\ .8 \end{bmatrix}$$

Using the parameter selection scheme developed in section 3.3.3, the new improved free parameters may be selected. In equation (4-7), the instantaneous A matrix is separated into the SK form.

$$A = -\begin{bmatrix} 1.333 & -.526 \\ -.526 & 1.68 \end{bmatrix} \begin{bmatrix} \frac{1}{C_{10}} & 0 \\ 0 & \frac{1}{C_{11}} \end{bmatrix}$$
 (4-7)

Choosing $\alpha=1$, β is calculated from equation (4-8).

$$\frac{1}{\beta} + \frac{\beta}{1} = \frac{4s_{11}s_{22}}{\det[S]} - 2 \tag{4-8}$$

Using equations (3-17) and (3-18), the optimal parameters are calculated to be

$$k_1 = \frac{1}{C_{10}} = \frac{1+2.1}{2(1.33)} = \frac{1.16}{2(1.33)}$$
 (4-9)

and

$$k_2 = \frac{1}{C_{11}} = \frac{(1+2.1)}{2(1.68)} = \frac{.52}{...}$$
 (4-10)

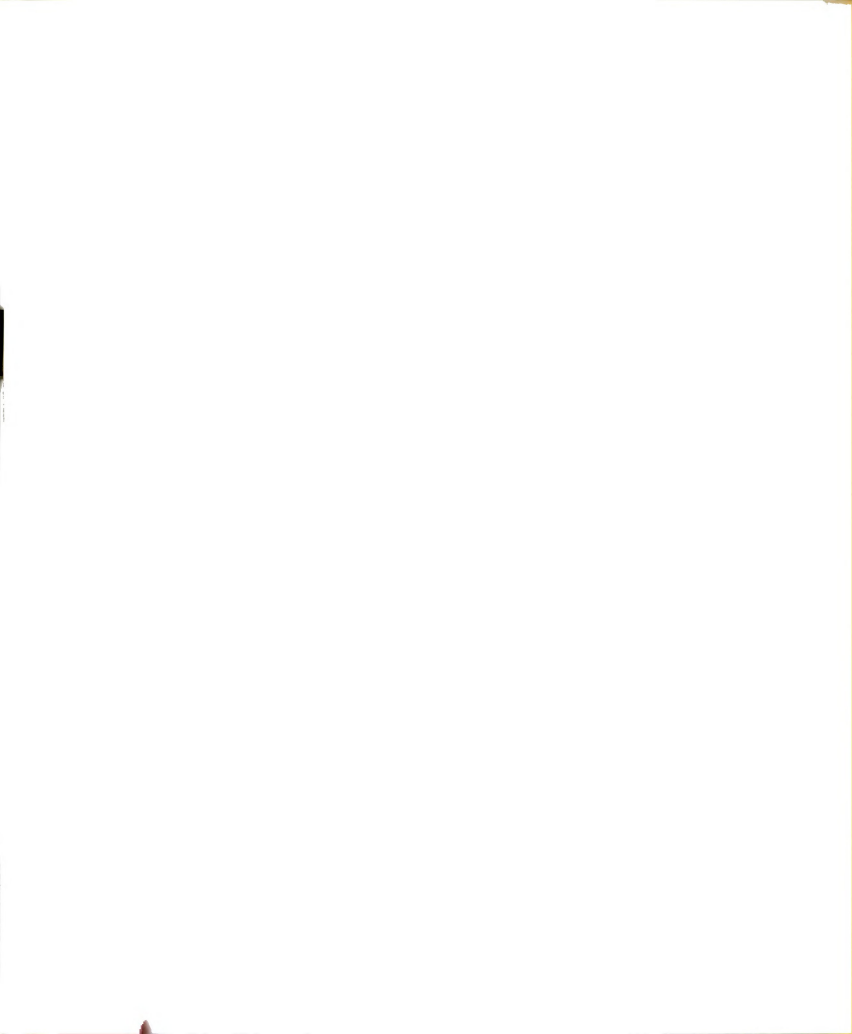


TABLE 4-1 Simulation Data

	Comments		Optimal Parameters	Optimal Parameters and respecified initial conditions
	ial tions	9 ₁₁ (0)	0.0	.7173
	Initial Conditions	910(0)	0.0	.774
	put tor	_	.9490162	.9490162
	Output Vector	E ₅ F ₆ 093	.949	.949
	State r	^ĝ 11 .373	. 6950	.6950
	Steady State Vector	⁹ 10 .898	.8182	.8182
	vative	^ۋ 11 0.0	0.0	0.0
	Derivativ Vector	•10 0.0	0.0	0.0
	Free meters*	k ₂	. 52	. 52
	Free Parameters*	k ₁	1.16	1.16
	Input Vector	E ₆	∞ .	ω .
	Inj Vec	Case F ₅ E ₆ 1 1.0 1.0	1.2 .8	1.2 .8
		Case 1	2	m

 $*k_1 = 1/C_{10}; k_2 = 1/C_{11}.$



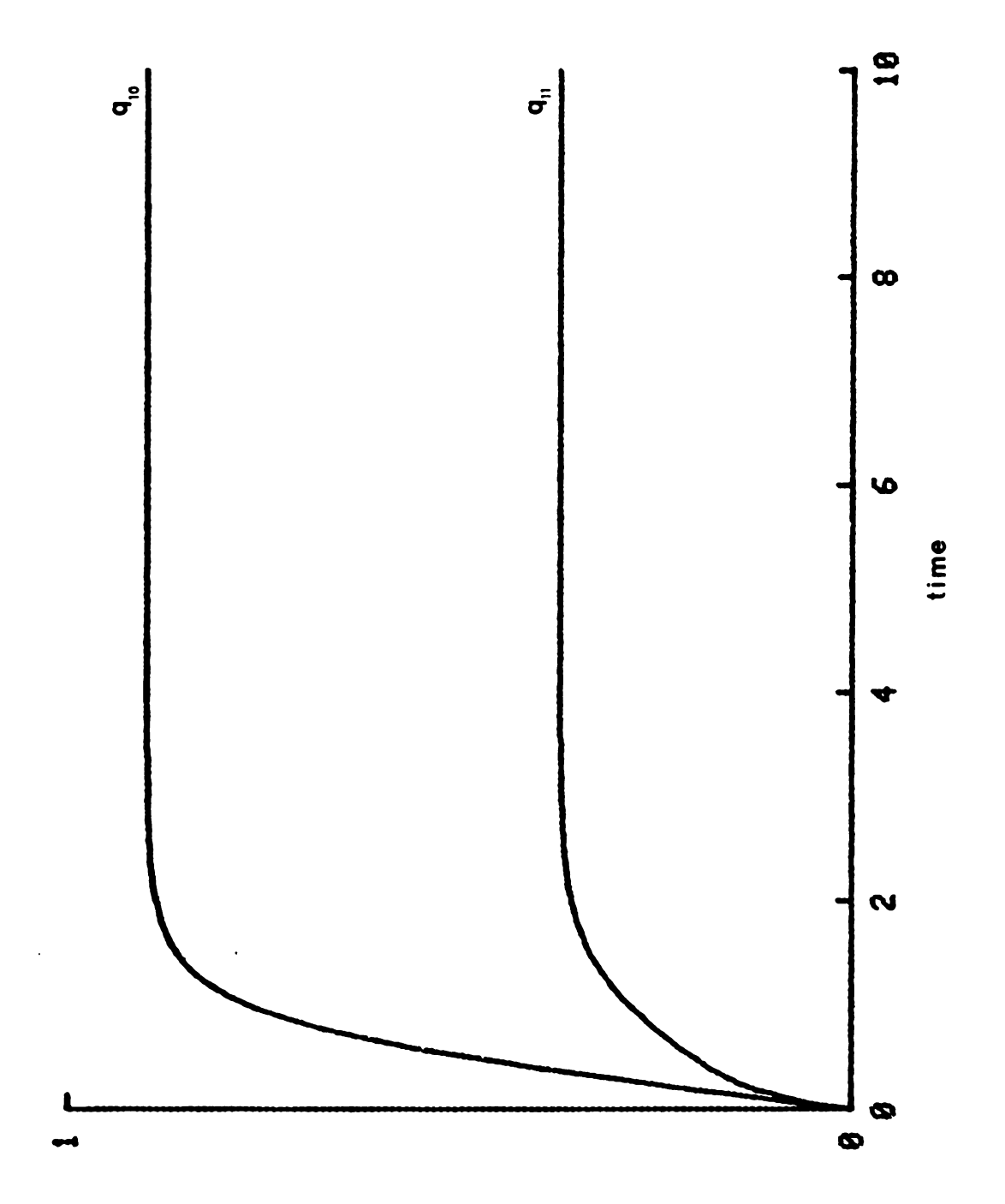


FIGURE 4-1. CASE 1

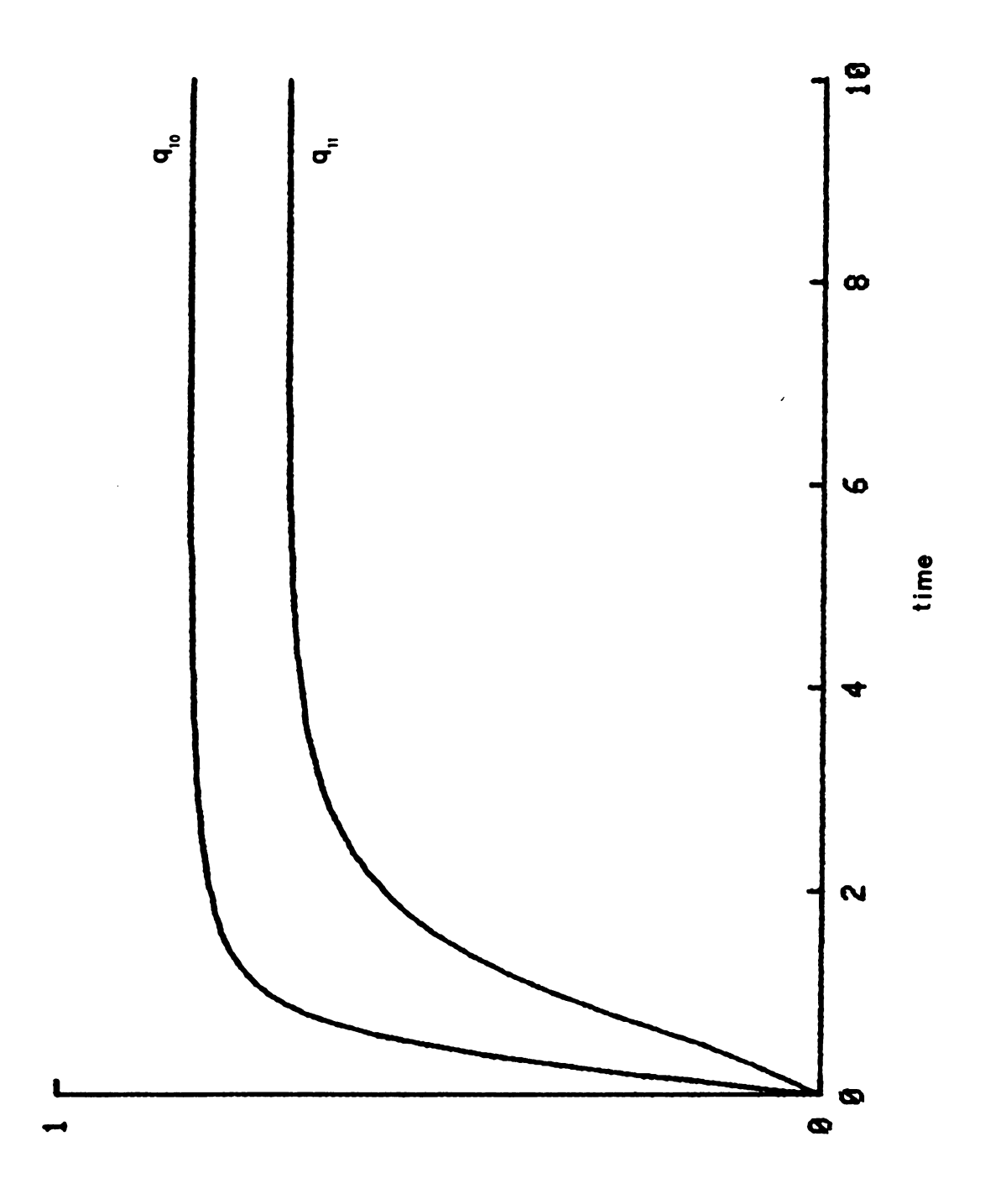
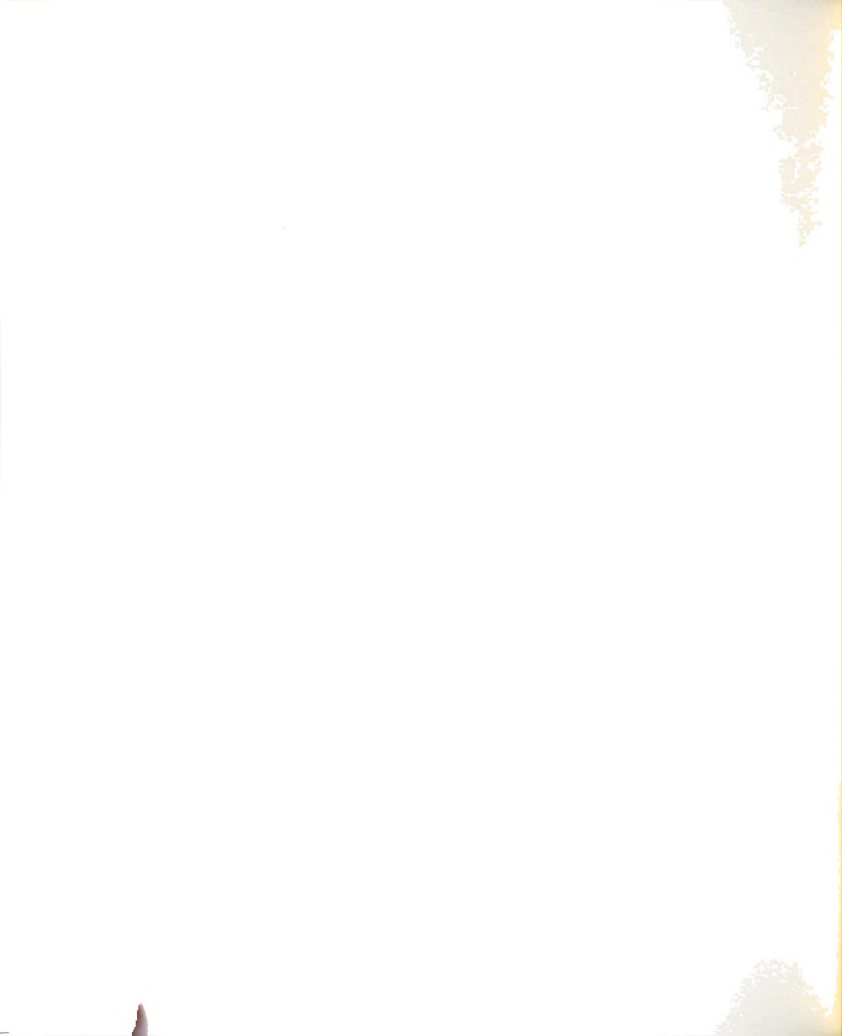
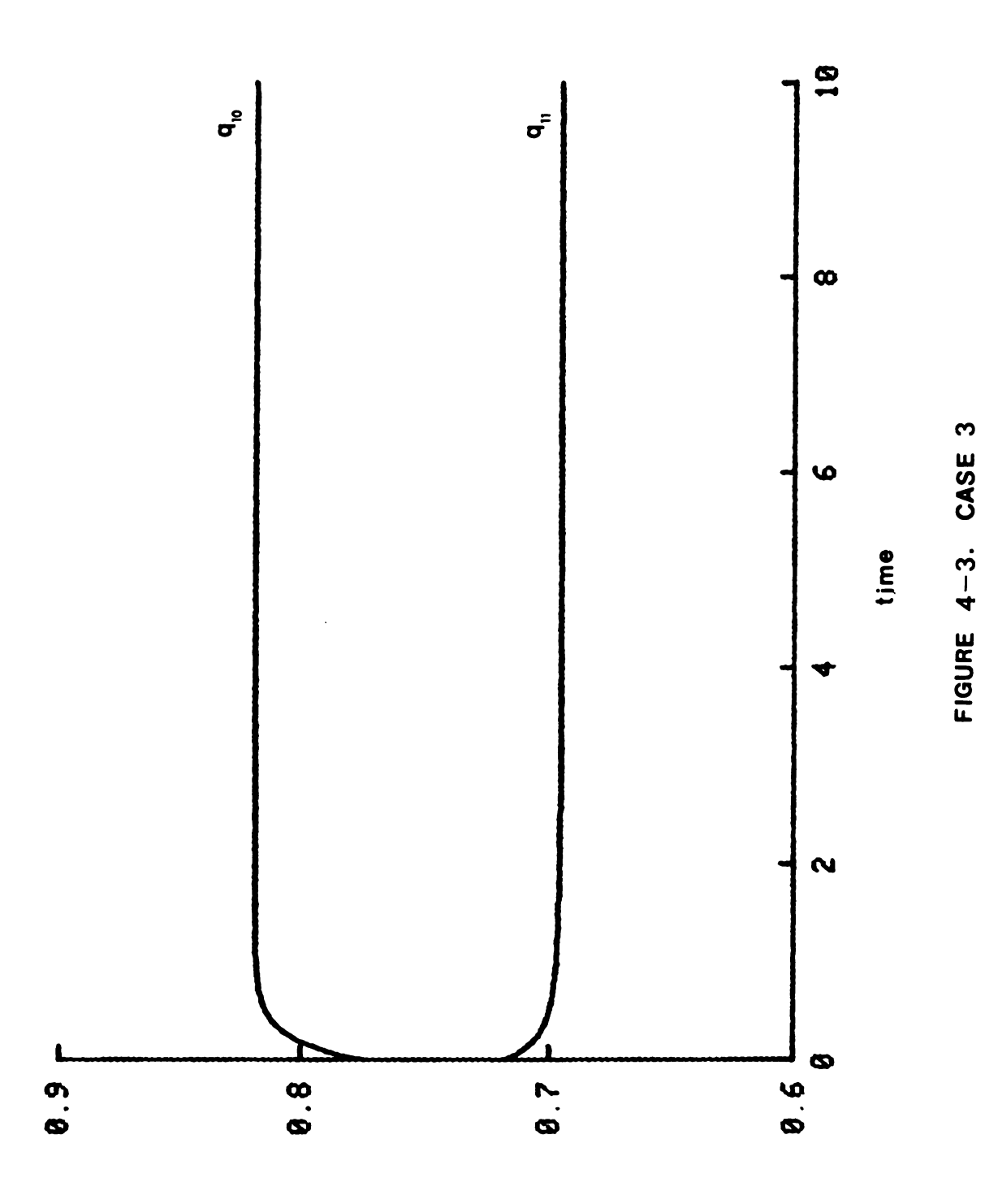


FIGURE 4-2. CASE 2







Figures 4-1 and 4-2 indicate no discernable difference in the time scales of response for the nonlinear system with the parameter equal to unity, and set to their optimal values. Tabulated in Table 4-2 are the approximating eigenvalues for these two cases. Evidently, the initial specification of C_{10} and C_{11} equal to unity was nearly optimal. Shown in Figure 4-3, is the convergence of the system to steady state with respecified initial conditions. Note that very few iterations are required. Table 4-1 tabulates the important information for each simulation.

TABLE 4-2 Eigenvalue Approximation

Cases	k ₁	k ₂	$^{\lambda}$ 1	$^{\lambda}2$	Comments
1	1.0	1.0	-2.065	9505	Default parameters
2	1.16	.52	-2.1	-1.0	Optimal parameters

4.2 Example 2

The augmented sub-graph used in example problem 1 is reconsidered here again; however, the dissipation functions have been redefined as follows:

$$f_1 = 6 \text{ TANH } (e_1)$$
 (4-11)

$$f_2 = 3 \text{ TANH } (e_2)$$
 (4-12)

$$f_3 = 3e_3^3 + 2e_3$$
 (4-13)

$$f_4 = \frac{15e_4}{9+e_4^2} \tag{4-14}$$



Figure 4-4 illustrates the nature of the dissipation functions.

Tabulated in Table 4-3 are the relevant data for Figures 4-5 and

4-6. In Table 4-4, the instantaneous eigenvalues for case 1 and

case 2 computed from the equivalent resistance method are compared.

Note in this example, the selection of the optimal parameter

provided a significant decrease in eigenvalue seperation (see

Table 4-4). In case 1, the input vector has been specified to be

$$\begin{bmatrix} F_5 \\ E_6 \end{bmatrix} = \begin{bmatrix} 8.0 \\ -2.0 \end{bmatrix} \tag{4-15}$$

In case 2, at the subsequent sub-system call, for the sake of example, the input vector has been assumed to be displaced to

$$\begin{bmatrix} F_5 \\ E_6 \end{bmatrix} = \begin{bmatrix} 7.9 \\ -1.95 \end{bmatrix} \tag{4-16}$$

from the information provided in case 1. The improved initial conditions for case 2 were calculated from the equation

$$x_{t_d}(0) = \hat{x}_{t_{d-1}}/k_{t_{d \text{ opt.}}}$$
 (4-17)

Apparent from Figure 4-6 is the rapid convergence of the system to the new steady-state effected by the choice of an optimal parameter pair and respecification of the initial conditions.



TABLE 4-3 Simulation Data

Comments		Default parameters and initial condi- tions	.6613 .3621 1.74 .296 .6822 .3702 Optimal parameters and respecified initial conditions
i) :ions	9 ¹¹ (0)	0.0	.3702
Initial Conditions	\hat{q}_{11} E ₅ F ₆ $q_{10}(0)$ $q_{11}(0)$.770 1.79 .30 0.0	.6822
t or	F ₆	.30	.296
Oupu Vect	E ₅	1.79	1.74
Steady State Ouput Vector Vector	â ₁₁	.770	.3621
Steady	⁹ 10	1.79	.6613
ative tor	• •	0.0	0.0 0.0
Derivative Vector	الهُ واهُ	0.0 0.0	0.0
Free Parameters*	k 2	1.0	2.08
Fr Parame	k ₁ k ₂	1.0 1.0	2.624 2.08
Input /ector	F ₅ E ₆	8.0 -2.0	7.9 -1.95
	F ₅	8.0	7.9
Case		-	2

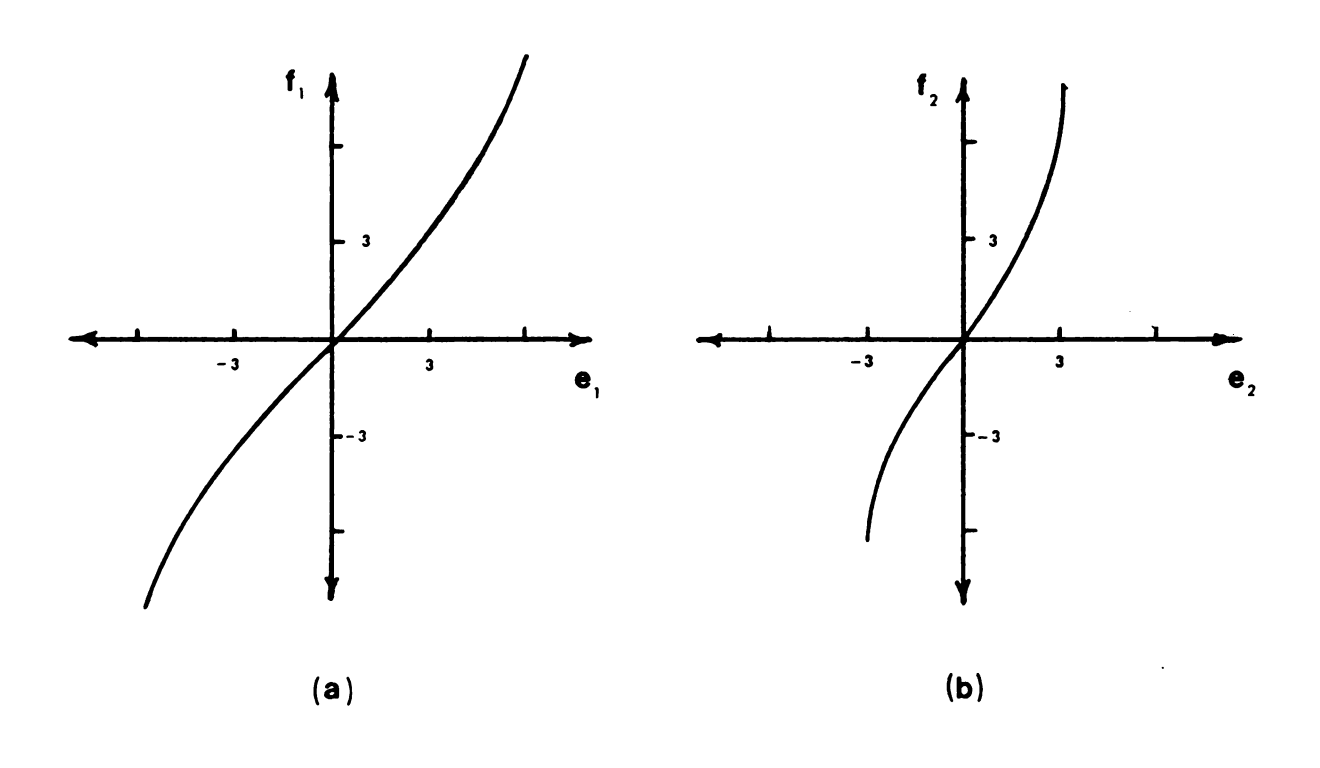
 $*k_1 = 1/C_{10}; k_2 = 1/C_{11}.$



TABLE 4-4 Eigenvalue Approximation

	k ₁	k ₂	λ ₁	λ2	Comments
Case 1	1.0	1.0	-35.77	884	Default parameters
Case 2	2.624	2.08	-27.25	-1.0	Optimal parameters





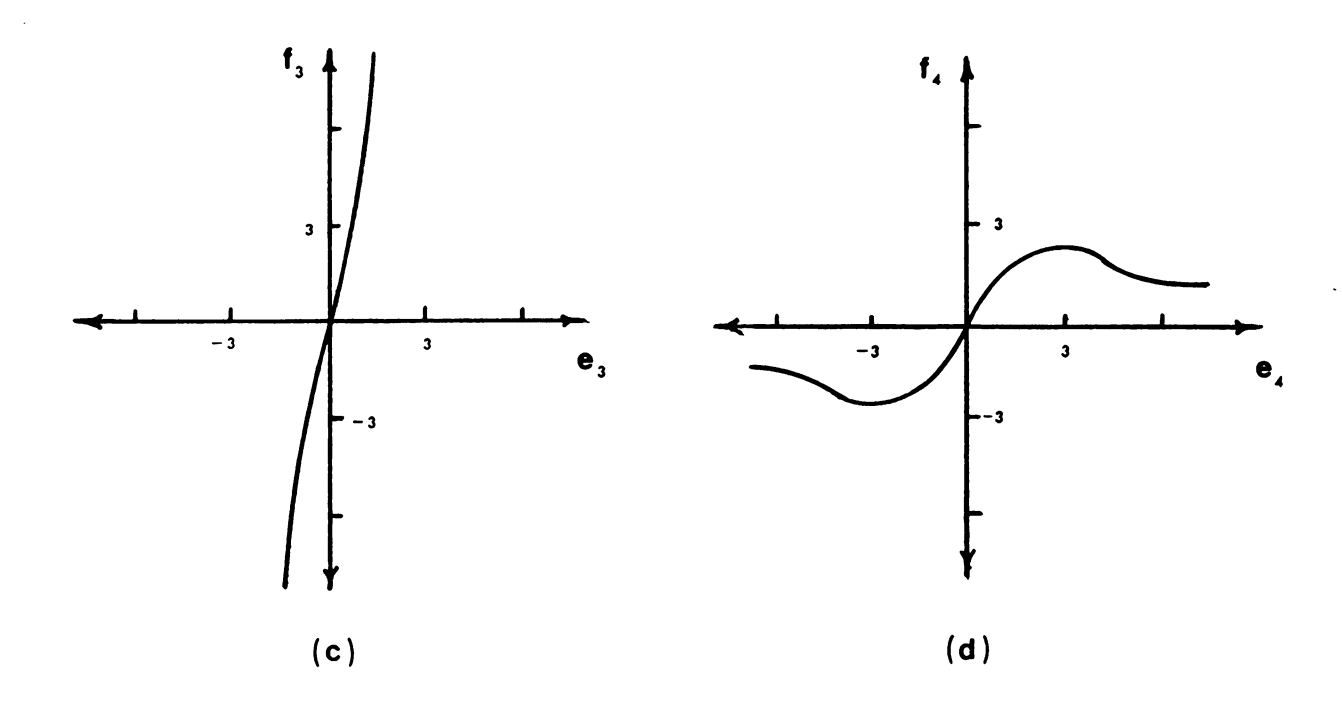
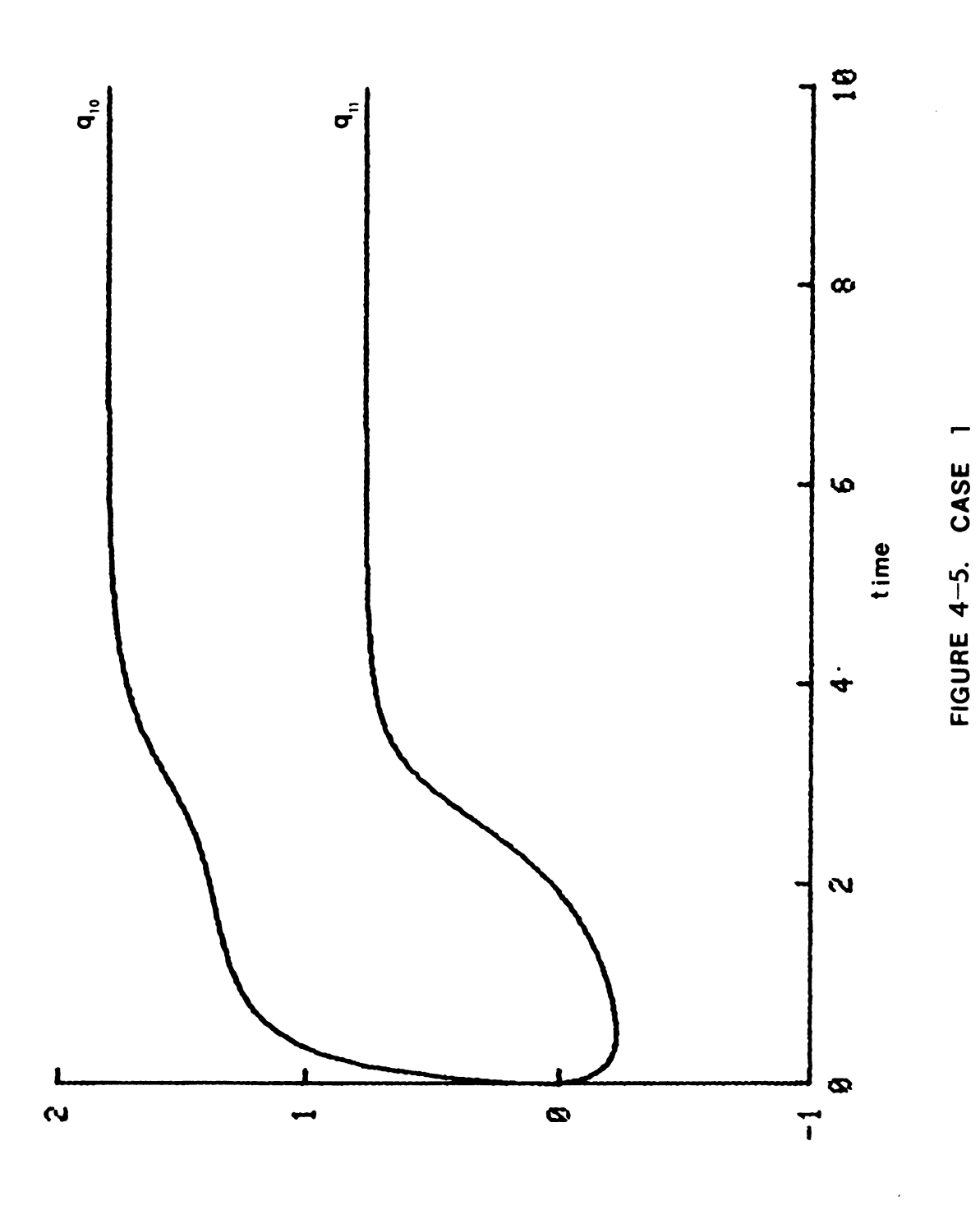
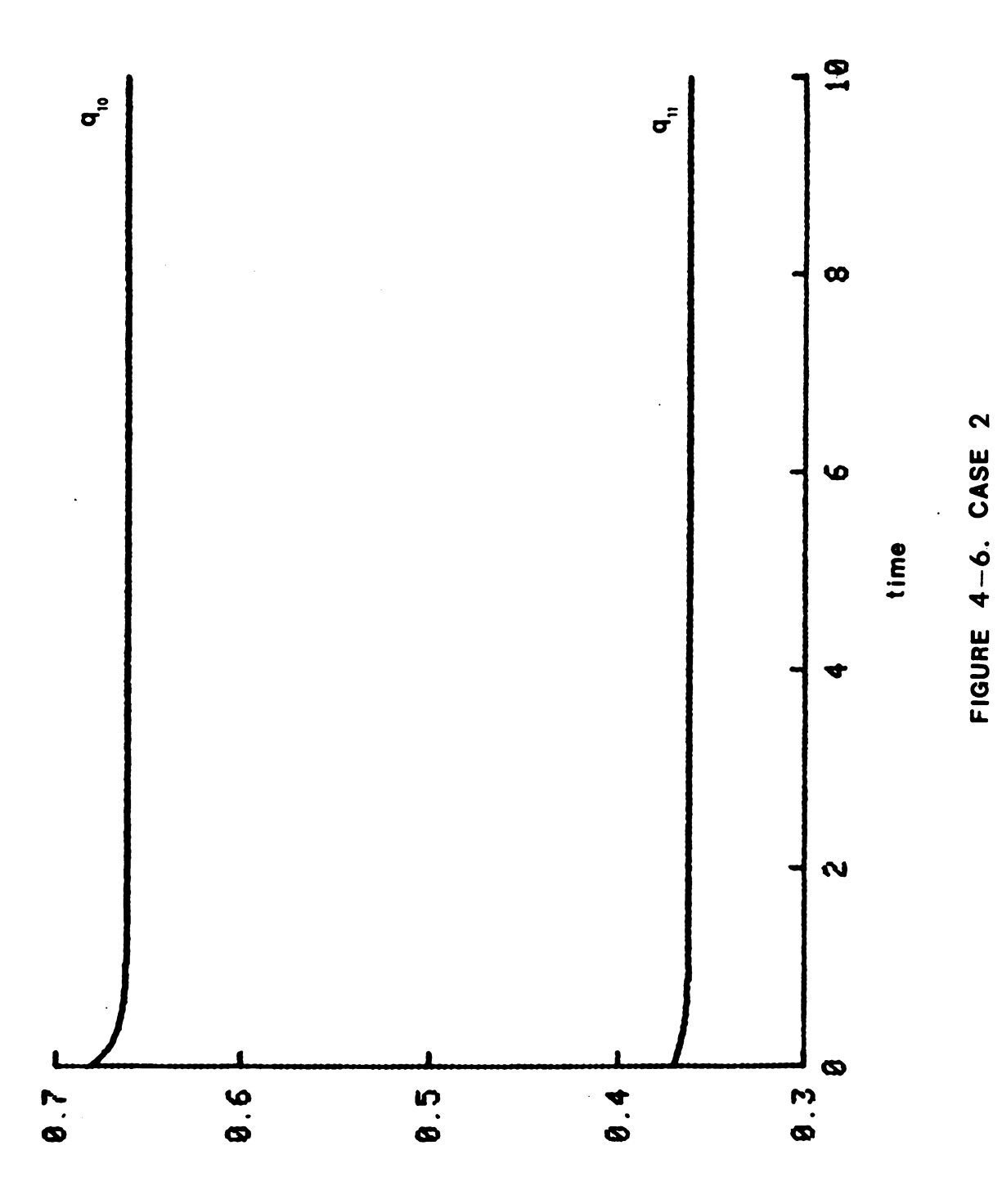


FIGURE 4-4. DISSIPATIVE FUNCTIONS FOR EXAMPLE 2











5.0 CONCLUSIONS

5.1 The General Problem Structure

In Figure 5-1, a diagram representing the general problem structure is illustrated. From this diagram, several alternate paths of investigation as well as potential directions for future work are shown.

5.2 Summary of Results

In the preceding chapters, the origin and identification of algebraic loops within the framework of the bond graph approach has been discussed. Following the identification of the bond-graph fragments containing algebraic loops, a procedure for the structural modification of the static sub-graphs containing the loops was defined. Inherent to this particular procedure is the concept of piecewise simulation.

Associated with the dynamic augmentation of the static subgraphs is the problem of parameter selection. A procedure for the selection of parameters for optimal pole placement in 1st and 2nd order linear systems has been outlined. By recasting the nonlinear problem into an approximate linear equivalent, the task of parameter selection was reduced to that for the linear problem.



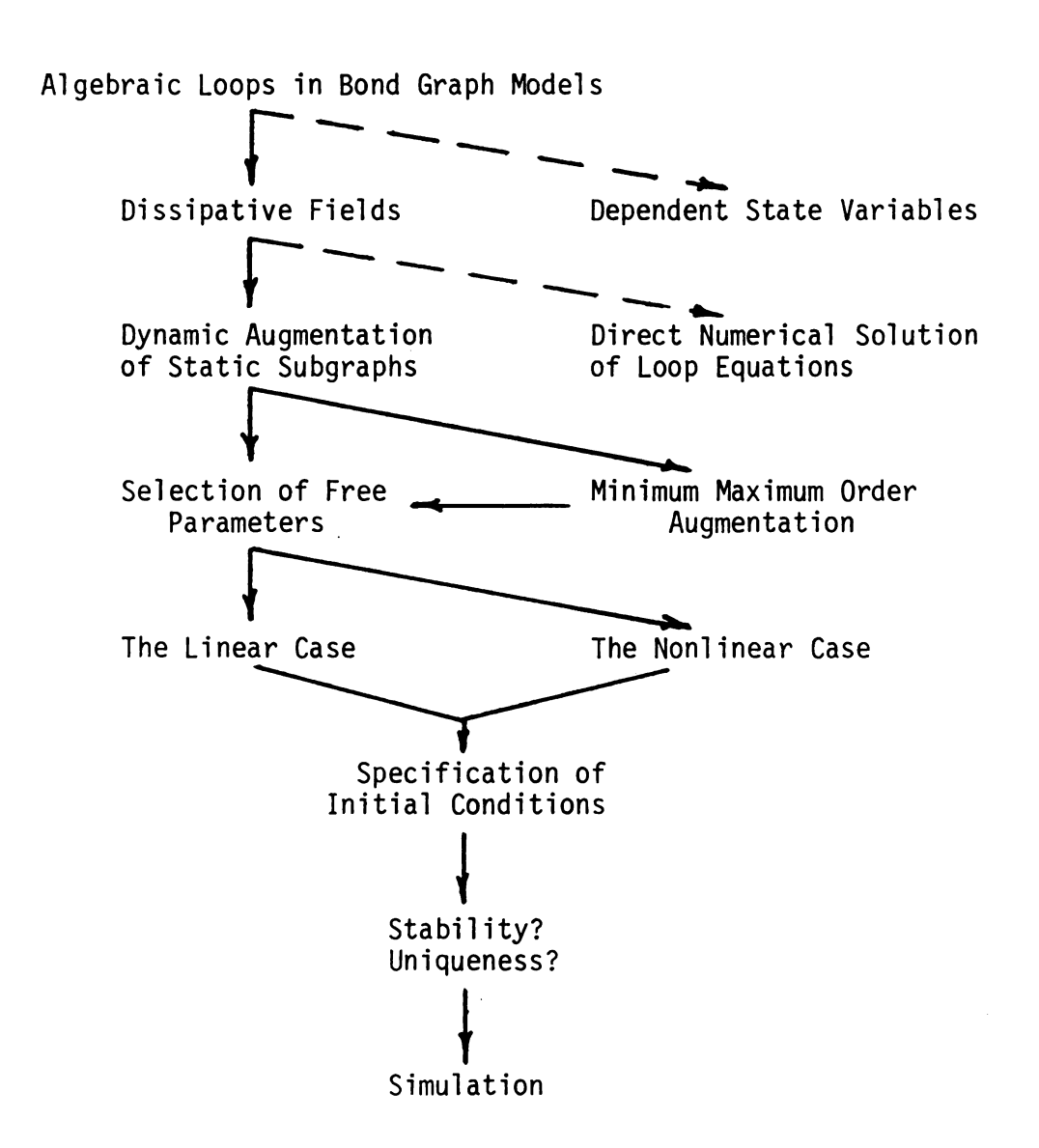


FIGURE 5-1. THE PROBLEM STRUCTURE



68

The solution process incorporating the required manipulations for a bond-graph model containing algebraic loops was delineated in a flowchart format.

Chapter 4 contains two numerical examples implementing the solution process. These examples demonstrate the viability of the solution process discussed in this thesis.

5.3 Open Questions

Remaining undetermined is the manner of selection of optimal parameters for a general nth order augmented sub-graph, and the associated stability question.

It may be remarked that for dissipation functions strictly increasing and confined to the 1st and 3rd quadrants of the effort-flow plane, as demonstrated in Figure 4-4, stability for a non-linear subsystem is ensured independent of parameter values, provided they are positive. In a physical sense, such a system disturbed by constant inputs will eventually settle to a steady-state where energy influx equates with energy dissipation. Further work however, should be pursued in examining system stability for a general class of dissipation functions with, for example, the capability of returning power to the system for finite time intervals.

Experience indicates that most physical systems represented by bond graph models containing algebraic loops may be adequately handled with only a lst or 2nd order augmentation. It remains desirable to develop an algorithm for the parameter selection for the general nth order case.



It must also be noted that the bond-graph model requires the dissipation functions to have an explicit form of either

$$e = \phi(f) \tag{5-1}$$

or

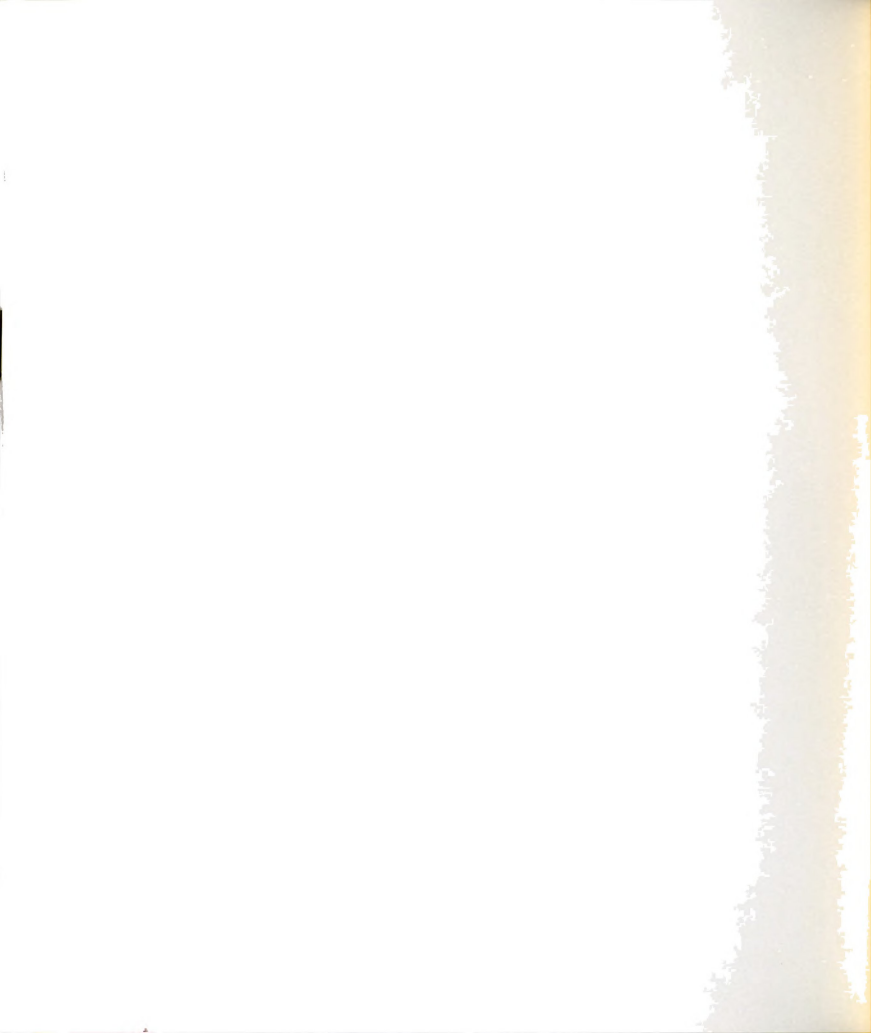
$$f = \psi(e) \tag{5-2}$$

Therefore, implicit forms of the dissipative functions are not addressed by the method of dynamic augmentation.

In summary, the utility of the method of dynamic augmentation of dissipative algebraic loops has been clearly demonstrated with bond graph techniques for a class of problems that were previously neglected.



APPENDIX



R. C. ROSENBERG

Associate Professor, Department of Mechanical Engineering, Michigan State University, East Lansing, Mich.

D. C. KARNOPP

Professor, Department of Mechanical Engineering, University of California, Davis, Calif.

A Definition of the Bond Graph Language

Introduction

THE purpose of this paper is to present the basic definitions of the bond graph language in a compact but general form. The language presented herein is a formal mathematical system of definitions and symbolism. The descriptive names are stated in terms related to energy and power, because that is the historical basis of the multiport concept.

It is important that the fundamental definitions of the language be standardized because an increasing number of people around the world are using and developing the bond graph language as a modeling tool in relation to multiport systems. A common set of reference definitions will be an aid to all in promoting ease of communication.

Some care has been taken from the start to construct definitions and notation which are helpful in communicating with digital computers through special programs, such as ENPORT [5]. It is hoped that any subsequent modifications and extensions to the language will give due consideration to this goal.

Principal sources of extended descriptions of the language and physical applications and interpretations will be found in Paynter [1], Karnopp and Rosenberg [2, 3], and Takahashi, et al. [4]. This paper is the most highly codified version of language definition, drawing as it does upon all previous efforts.

Basic Definitions

Multiport Elements, Ports, and Bonds. Multiport elements are the nodes of the graph, and are designated by alpha-numeric characters. They are referred to as elements, for convenience. For example, in Fig. 1(a) two multiport elements, 1 and R, are shown. Ports of a multiport element are designated by line

segments incident on the element at one end. Ports are places where the element can interact with its environment.

For example, in Fig. 1(b) the 1 element has three ports and the R element has one port. We say that the 1 element is a 3-port, and the R element is a 1-port.

Bonds are formed when pairs of ports are joined. Thus bonds are connections between pairs of multiport elements.

For example, in Fig. 1(c) two ports have been joined, forming a bond between the 1 and the R.

Bond Graphs. A bond graph is a collection of multiport elements bonded together. In the general sense it is a linear graph whose nodes are multiport elements and whose branches are bonds.

A bond graph may have one part or several parts, may have no loops or several loops, and in general has the characteristics of any linear graph.

An example of a bond graph is given in Fig. 2. In part (a) a bond graph with seven elements and six bonds is shown. In part (b) the same graph has had its powers directed and bonds labeled.

A bond graph fragment is a bond graph not all of whose ports have been paired as bonds.

An example of a bond graph fragment is given in Fig. 1(c), which has one bond and two open, or unconnected, ports.

Port Variables. Associated with a given port are three direct and three integral quantities.

Effort, e(t), and flow, f(t), are directly associated with a given port, and are called the port power variables. They are assumed to be scalar functions of an independent variable (t).

Power, P(t), is found directly from the scalar product of effort and flow, as

$$P(t) = e(t) \cdot f(t).$$

The direction of positive power is indicated by a half-arrow on the bond.

Momentum, p(t), and displacement, q(t), are related to the effort and flow at a port by integral relations. That is,

¹Numbers in brackets designate References at end of paper.

Contributed by the Automatic Control Division for publication (without presentation) in the JOURNAL OF DYNAMIC STETMS, MEASUREMENT, AND CONTROL. Manuscript received at ASME Headquarters, May 9, 1972. Paper No. 72-Aut-T.

Copies will be available until September, 1973.

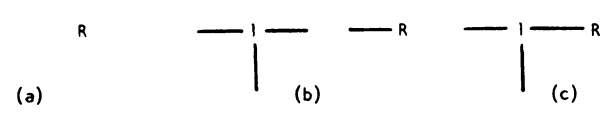


Fig. 1 Multiport elements, ports, and bonds: (a) two multiport elements; (b) the elements and their ports; (c) formation of a bond

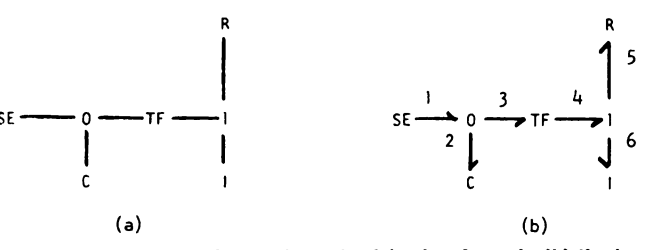


Fig. 2 An example of a bond graph: (a) a bond graph; (b) the bond graph with powers directed and bonds labeled

$$p(t) = p(t_0) + \int_{t_0}^{t} e(\lambda) d\lambda$$

and
$$q(t) = q(t_0) + \int_{t_0}^{t} f(\lambda) d\lambda$$
, respectively.

Momentum and displacement are sometimes referred to as energy variables.

Energy, E(t), is related to the power at a port by

$$E(t) = E(t_0) + \int_{t_0}^{t} P(\lambda) d\lambda.$$

The quantity $E(t) - E(t_0)$ represents the net energy transferred through the port in the direction of the half-arrow (i.e., positive power) over the interval (t_0, t) .

In common bond graph usage the effort and the flow are often shown explicitly next to the port (or bond). The power, displacement, momentum, and energy quantities are all implied.

Basic Multiport Elements. There are nine basic multiport elements, grouped into four categories according to their energy characteristics. These elements and their definitions are summarized in Fig. 3.

Saurces

Source of effort, written SE \underline{e} , is defined by e = e(t). Source of flow, written SF \underline{f} , is defined by f = f(t).

Storages.

Capacitance, written $\frac{e}{f}$ C, is defined by

$$e = \Phi(q)$$
 and $q(t) = q(t_0) + \int_{t_0}^{t} f(\lambda)d\lambda$.

That is, the effort is a static function of the displacement and the displacement is the time integral of the flow.

Inertance, written $\frac{e}{f}I$, is defined by

$$f = \Phi(p)$$
 and $p(t) = p(t_0) + \int_{t_0}^{t} e(\lambda) d\lambda$.

That is, the flow is a static function of the momentum and the momentum is the time integral of the effort.

Dissipation.

Resistance, written $\frac{e}{f}R$, is defined by

$$\Phi(e,f)=0.$$

SYMBOL	DEFINITION	NAME
SE — e — sr — f	e = e(t) $f = f(t)$	source of effort
c <u>e</u>	$e = \Phi(q)$	capacitance
l <mark>∉ e</mark> f	$q(t) = q(t_0) + \int f \cdot dt$ $f = \Phi(p)$ $p(t) = p(t_0) + \int e \cdot dt$	inertance
R ℓ e f	$\Phi(e,f) = 0$	resistance
1 TF 2	e ₁ = m·e ₂ m·f ₁ = f ₂	transformer
-1 GY -2	e ₁ = r·f ₂ e ₂ = r·f ₁	gyrator
$\frac{1}{12}0\frac{3}{12}$	$e_1 = e_2 = e_3$ $f_1 + f_2 - f_3 = 0$	common effort junction
1 3	$f_1 = f_2 = f_3$ $e_1 + e_2 - e_3 = 0$	common flow junction

Fig. 3 Definitions of the basic multiport elements

That is, a static relation exists between the effort and flow at the port.

Junctions: 2-Port.

Transformer, written $\frac{e_1}{f_1}$ TF $\frac{e_2}{f_2}$, is a linear 2-port element defined by

$$e_1 = m \cdot e_2$$

and

$$m \cdot f_1 = f_2,$$

where m is the modulus.

Gyrator, written $\frac{e_1}{f_1}$ GY $\frac{e_2}{f_2}$, is a linear 2-port element defined by

$$e_1 = r \cdot f_2$$

and

$$e_2 = r \cdot f_1,$$

where r is the modulus.

Both the transformer and gyrator preserve power (i.e., $P_1 = P_2$ in each case shown), and they must each have two ports, so they are called essential 2-port junctions.

Junctions: 3-Port.

Common effort junction, written $\frac{1}{2}$ O $\frac{3}{2}$

is a linear 3-port element defined by

$$e_1 = e_2 = e_3$$
 (common effort)

and

$$f_1 + f_2 - f_3 = 0.$$
 (flow summation)

Other names for this element are the flow junction and the



zero junction. Common flow junction, written $\frac{1}{2}$ 1 $\frac{3}{2}$

is a linear 3-port element defined by

$$f_1 = f_2 = f_3$$
 (common flow)

and

$$e_1 + e_2 - e_3 = 0.$$
 (effort summation)

Other names for this element are the effort junction and the one junction.

Both the common effort junction and the common flow junction preserve power (i.e., the *nct* power in is zero at all times), so they are called junctions. If the reference power directions are changed the signs on the summation relation must change accordingly.

Extended Definitions

Multiport Fields.

Storage Fields. Multiport capacitances, or C-fields, are written

$$\frac{1}{2}$$
 $C \stackrel{n}{\longleftarrow}$, and characterized by

$$e_i = \Phi_i(q_1, q_2, \ldots, q_n), i = 1 \text{ to } n,$$

and
$$q_i(t) = q_i(t_0) + \int_{t_0}^t f_i(\lambda) d\lambda$$
, $i = 1$ to n .

Multiport inertances, or I-fields, are written $\frac{1}{2}I \stackrel{n}{\smile}$,

and characterized by

$$f_i = \Phi_i(p_1, p_2, \dots p_n), i = 1 \text{ to } n,$$
 and
$$p_i(t) = p_i(t_0) + \int_{t_0}^t e_i(\lambda) d\lambda, i = 1 \text{ to } n.$$

If a C-field or I-field is to have an associated "energy" state function then certain integrability conditions must be met by the Φ_i functions. In multiport terms the relations given in the foregoing are sufficient to define a C-field and I-field, respectively.

Mixed multiport storage fields can arise when both C and I-type storage effects are present simultaneously. The symbol for such an element consists of a set of C's and I's with appropriate ports indicated.

For example, $\frac{1}{2}ICI\frac{3}{2}$ indicates the existence of a set

of relations

$$f_1 = \Phi_1(p_1, q_2, p_3),$$

$$c_2 = \Phi_2(p_1, q_2, p_3),$$

$$f_3 = \Phi_3(p_1, q_2, p_3),$$

and

$$p_{1}(t) = p_{1}(t_{0}) + \int_{t_{0}}^{t} e_{1}(\lambda)d\lambda,$$

$$q_{2}(t) = q_{2}(t_{0}) + \int_{t_{0}}^{t} f_{2}(\lambda)d\lambda,$$

$$p_{3}(t) = p_{3}(t_{0}) + \int_{t_{0}}^{t} e_{3}(\lambda)d\lambda.$$

Multiport dissipators, or R-fields, are written $\frac{1}{2}$ R $\frac{n}{2}$

and are characterized by

$$\Phi_i(e_1, f_1, e_2, f_2, \ldots e_n, f_n) = 0, i = 1 \text{ to } n.$$

If the R-field is to represent pure dissipation, then the power function associated with the R-field must be positive definite.

Multiport junctions include 0 junctions and 1 - junctions with n ports, $n \geq 2$. The general case for each junction is given in the following.

Modulated 2-Port Junctions. The modulated transformer, or

$$MTF$$
 written $\frac{1}{m(\mathbf{x})}$ implies the realtions $e_1 = m(\mathbf{x}) \cdot e_2$

and $m(\mathbf{x}) \cdot f_1 = f_2$

where m(x) is a function of a set of variables, x. The modulated transformer preserves power; i.e., $P_1(t) = P_2(t)$.

The modulated gyrator, or MGY, written $\frac{r(x)}{1}$ $\frac{MGY}{2}$ implies the relations

$$\epsilon_1 = r(\mathbf{x}) \cdot f_2$$

$$\epsilon_2 = r(\mathbf{x}) \cdot f_1$$

where r(x) is a function of set of variables, x. The modulated gyrator preserves power; i.e., $P_1(t) = P_2(t)$.

Junction Structure. The junction structure of a bond graph is the set of all 0, 1, GY, and TF elements and their bonds and ports. The junction structure is an *n*-port that preserves power (i.e., the *net* power in is zero). The junction structure may be modulated (if it contains any MGY's or MTF's) or unmodulated.

For example, the junction structure of the graph in Fig. 2(b) is a 4-port element with ports 1, 2, 5, and 6 and bonds 3 and 4. It contains the elements 0, TF, and 1.

Physical Interpretations

The physical interpretations given in this section are very succinctly stated. References [1], [2], and [3] contain extensive descriptions of physical applications and the interested reader is encouraged to consult them.

Mechanical Translation. To represent mechanical translational phenomena we may make the following variable associations:

- 1 effort, e, is interpreted as force;
- 2 flow, f, is interpreted as velocity;
- 3 momentum, p, is interpreted as impulse-momentum;
- 4 displacement, q, is interpreted as mechanical displacement.

Then the basic bond graph elements have the following interpretations:

- 1 source of effort, SE, is a force source;
- 2 source of flow, SF, is a velocity source (or may be thought of as a geometric constraint);



- 3 resistance, R, represents friction and other mechanical loss mechanisms;
- 4 capacitance, C, represents potential or elastic energy storage effects (or spring-like behavior);
- 5 inertance, I, represents kinetic energy storage (or mass effects);
- 6 transformer, TF, represents linear lever or linkage action (motion restricted to small angles);
- 7 gyrator, GY, represents gryational coupling or interaction between two ports;
- 8 0-junction represents a common force coupling among the several incident ports (or among the ports of the system bonded to the 0-junction); and
- 9 1-junction represents a common velocity constraint among the several incident ports (or among the ports of the system bonded to the 1-junction).

The extension of the interpretation to rotational mechanics is a natural one. It is based on the following associations:

- 1 effort, e, is associated with torque; and
- 2 flow, f, is associated with angular velocity.

Because the development is so similar to the one for translational mechanics it will not be repeated here.

Electrical Networks. In electrical networks the key step is to interpret a port as a terminal-pair. Then variable associations may be made as follows:

- 1 effort, e, is interpreted as voltage;
- 2 flow, f, is interpreted as current;
- 3 momentum, p, is interpreted as flux linkage;
- displacement, q, is interpreted as charge.

The basic bond graph elements have the following interpretations:

- 1 source of effort, SE, is a voltage source;
- source of flow, SF is a current source; 2
- 3 resistance, R, suprements electrical resistance;
- capacitance, C. represents capacitance effect (stored electric energy);
- 5 inertance, I, septements inductance (stored magnetic energy);
 - transformer, A.T. Expresents ideal transformer coupling;
 - gyrator, GY, represents gyrational coupling;
- 0-junction regressions a parallel connection of ports (common voltage across the imminal pairs); and
- 9 1-junction represents a series connection of ports (common current through the terminal pairs).

Hydraulic Circuits. For fluid systems in which the significant fluid power is given as the product of pressure times volume flow, the following variable associations are useful:

- 1 effort, e, is interpreted as pressure;
- 2 flow, f, is interpreted as volume flow.
- 3 momentum, p, is interpreted as pressure-momentum;
- displacement, q, is interpreted as volume.

The basic bond graph elements have the following interpretations:

- 1 source of effort, SE, is a pressure source;
- source of flow, SF, is a volume flow source;

- 3 resistance, R, represents loss effects (e.g., due to leakage, valves, orifices, etc.);
- 4 capacitance, C, represents accumulation or tank-like effects (head storage);
 - 5 inertance, I, represents slug-flow inertia effects:
- 6 0-junction represents a set of ports having a common pressure (e.g., a pipe tee);
- 7 1-junction represents a set of ports having a common volume flow (i.e., series).

Other Interpretations. This brief listing of physical interpretations of bond graph elements is restricted to the simplest, most direct, applications. Such applications came first by virtue of historical development, and they are a natural point of departure for most classically trained scientists and engineers. As references [1-4] and the special issue collection in the JOURNAL OF DYNAMIC SYSTEMS, MEASUREMENT, AND CON-TROL, TRANS. ASME, Sept. 1972, indicate, bond graph elements can be used to describe an amazingly rich variety of complex dynamic systems. The limits of applicability are not bound by energy and power in the sense of physics; they include any areas in which there exist useful analogous quantities to energy.

Concluding Remarks

In this brief definition of the bond graph language two important concepts have been omitted. The first is the concept of hond activation, in which one of the two power variables is suppressed, producing a pure signal coupling in place of the bond. This is very useful modeling device in active systems. Further discussion of activation will be found in reference [3], section 2.4, as well as in references [1] and [2].

Another concept omitted from discussion in this definitional paper is that of operational causality. It is by means of causality operations applied to bond graphs that the algebraic and differential relations implied by the graph and its elements may be organized and reduced to state-space form in a systematic manner. Extensive discussion of causality will be found in reference [3], section 3.4 and chapter 5. Systematic formulation of relations is presented in reference [6].

References

- 1 Paynter, H. M., Analysis and Design of Engineering Systems, M.I.T. Press, 1961.
 2 Karnopp. D. C., and Rosenberg, R. C., Analysis and Simulation of Multiport Systems, M.I.T. Press, 1968.
- 3 Karnopp, D. C., and Rosenberg, R. C., "System Dynamics: A Unified Approach," Division of Engineering Research, College of Engineering, Michigan State University, East Lansing, Mich., 1971.
- 4 Takahaski, Y., Rabins, M., and Auslander, D., Control, Addison-Wesley, Reading, Ma., 1970 (see chapter 6 in particular).
- 5 Rosenberg, R. C., "ENPORT User's Guide," Division of Engineering Research, College of Engineering, Michigan State
- University, East Lansing, Mich., 1972.
 6 Rosenberg, R. C., "State-Space Formulation for Bond Graph Models of Multiport Systems," JOURNAL OF DYNAMIC SYSTEMS, MEASUREMENT, AND CONTROL, TRANS. ASME, Series G, Vol. 93, No. 1, Mar. 1971, pp. 35-40.



APPENDIX A2

Mathematical Basis for Dynamic Augmentation

The incidence of algebraic loops, within the framework of the bond-graph approach, are associated with acausal fragments as has been shown. Let us reconsider the acausal static sub-graph shown again in Figure 2-5c. By virtue of the nature of the junction elements, the following statements can be made:

$$\Sigma$$
 efforts = 0 'l' junction (A-1)

$$\Sigma$$
 flows = 0 '0' junction (A-2)

For the augmented sub-graph, the following statements can be made:

$$\Sigma$$
 efforts = \dot{p} 'l' junction (A-3)

$$\Sigma$$
 flows = \dot{x} '0' junction (A-4)

The condition of steady-state requires that

$$\begin{bmatrix} \dot{p} \\ \dot{x} \end{bmatrix} = \begin{bmatrix} 0 \\ 0 \end{bmatrix} \tag{A-5}$$



Consequently, at steady-state, the junction imposed constraint equations of the dynamic system are

$$\Sigma$$
 efforts = 0 '1' junctions (A-6)

$$\Sigma$$
 flows = 0 '0' junctions (A-7)

From this result, it is evident that the algebraic character of the static sub-graph is preserved at the steady-state of a properly augmented sub-graph. Note that augmentation can be extended to any or all of the '0' and '1' junctions contained within a static sub-graph.



LIST OF REFERENCES



REFERENCES

- 1. D. Karnopp and R. Rosenberg, "System Dynamics: A Unified Approach", N.Y., John Wiley & Sons, 1975.
- 2. L.G. Kelly, "Handbook of Numerical Methods and Applications", Reading, Mass., Addison-Wesley, 1967.
- 3. J.C. Bowers and S.R. Sedore, "SCEPTRE", Englewood Cliffs, New Jersey, Prentice-Hall, 1971.
- 4. G.A. Korn, J.V. Wait, "Digital Continuous System Simulations", Englewood Cliffs, New Jersey, Prentice-Hall, 1978.
- 5. R.N. Nilsen, "CSSL-IV", Chatsworth, CA., Simulation Services, 1977.
- 6. "CSMP III", White Plains, NY, IBM, 1975.
- 7. J.L. Meriam, "Dynamics", N.Y., John Wiley & Sons, 1971.
- 8. L. Meirovitch, "Analytical Methods in Vibration", N.Y., MacMillan Co., 1967.
- 9. R.A. Rohrer, "Circuit Theory: An Introduction to the State Variable Approach", N.Y., McGraw-Hill, 1970.
- 10. R.W. Brockett, "Finite Dimensional Systems", N.Y., John Wiley & Sons, 1969.









